Materials Chemistry and Physics 270 (2021) 124751

Contents lists available at ScienceDirect

Materials Chemistry and Physics

journal homepage: www.elsevier.com/locate/matchemphys

Investigating the effects of chitosan solution and chitosan modified TiO_2 nanotubes on the corrosion protection performance of epoxy coatings

Sepideh Pourhashem [a,b,c], Jizhou Duan [a,b,c,*], Ziyang Zhou [a,b,c,d], Xiaohong Ji [a,b,c], Jiawen Sun [a,b], Xucheng Dong [a,b], Lifei Wang [a,b], Fang Guan [a,b,c], Baorong Hou [a,b,c]

[a] Key Laboratory of Marine Environmental Corrosion and Bio-fouling, Institute of Oceanology, Chinese Academy of Sciences, 7 Nanhai Road, Qingdao, 266071, China
[b] Open Studio for Marine Corrosion and Protection, Pilot National Laboratory for Marine Science and Technology, 1 Wenhai Road, Qingdao, 266237, China
[c] Center for Ocean Mega-Science, Chinese Academy of Sciences, 7 Nanhai Road, Qingdao, 266071, PR China
[d] University of Chinese Academy of Sciences, 19 (Jia) Yuquan Road, Beijing, 100039, China

HIGHLIGHTS

- Synthesis of TiO_2 nanotubes modified with aqueous chitosan solution (TCS).
- Slight increase in corrosion resistance of epoxy by adding 2.5 wt% chitosan.
- Slight increase in corrosion resistance of epoxy by adding 0.1 wt% TCS.
- High corrosion resistance by simultaneously using chitosan and TCS in epoxy.

GRAPHICAL ABSTRACT

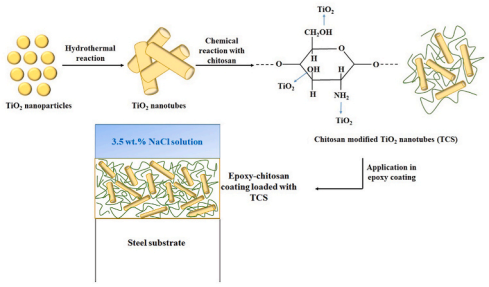

ARTICLE INFO

Keywords:
Epoxy
Chitosan
TiO_2 nanotubes
Nanocomposite coatings
Corrosion resistance

ABSTRACT

In this research, TiO_2 nanotubes (TNT) are hydrothermally synthesized and modified by chitosan (named as TCS). The structures of the prepared nanomaterials are investigated by X-ray diffraction and X-ray photoelectron spectroscopy, while transmission electron microscopy is used for characterizing the morphology of the nanopowders. Moreover, epoxy coatings loaded with different wt.% of TCS (0.1, 0.5, and 1.0 wt%), aqueous chitosan solution (1 and 2.5 wt%), and both aqueous chitosan solution (2.5 wt%) and TCS (0.1, 0.25, 0.5, and 1.0 wt%

Abbreviations: Chitosan modified TiO_2 nanotubes, TCS; Constant phase element of coating, CPE_{coat}; Constant phase element of corrosion products, CPE_{diff}; Constant phase element of double layer, CPE_{dl}; Electrochemical impedance spectroscopy, EIS; Epoxy coatings modified with chitosan, ECS; Epoxy coatings modified with 1 wt% of chitosan solution, ECS1%; Epoxy coatings modified with 2.5 wt% of chitosan solution, ECS2.5%; Epoxy coatings modified with 2.5 wt% of chitosan solution and loaded with 0.1 wt% of TCS, ECS-TCS0.1%; Epoxy coatings modified with 2.5 wt% of chitosan solution and loaded with 0.25 wt% of TCS, ECS-TCS0.25%; Epoxy coatings modified with 2.5 wt% of chitosan solution and loaded with 0.5 wt% of TCS, ECS-TCS0.5%; Epoxy coatings modified with 2.5 wt% of chitosan solution and loaded with 1.0 wt% of TCS, ECS-TCS1.0%; Field emission scanning electron microscopy, FE-SEM; Low-frequency impedance modulus, $|Z|_{0.01Hz}$; Low-frequency impedance modulus for nanocomposite coatings, $|Z|_{0.01Hz}^{nanocomposite\ coating}$; Low-frequency impedance modulus for pure polymer coating, $|Z|_{0.01Hz}^{pure\ coating}$; Open circuit potential, OCP; Resistance against charge transfer, R_{ct}; Resistance of coating, R_{coat}; Resistance of corrosion products, R_{diff}; Resistance of solution, R_s; Room temperature, T_{room}; TiO_2 nanotubes, TNT; Transmission electron microscopy, TEM; X-ray photoelectron spectroscopy, XPS; X-ray powder diffraction, XRD.

* Corresponding author. Key Laboratory of Marine Environmental Corrosion and Bio-fouling, Institute of Oceanology, Chinese Academy of Sciences, 7 Nanhai Road, Qingdao, 266071, China.
E-mail address: duanjz@qdio.ac.cn (J. Duan).

https://doi.org/10.1016/j.matchemphys.2021.124751
Received 17 February 2021; Received in revised form 19 April 2021; Accepted 19 May 2021
Available online 23 May 2021

TCS) are prepared which are abbreviated as E-TCS, ECS, and ECS-TCS coating systems, respectively. The corrosion behavior of the coated samples are considered by using salt spray and electrochemical impedance spectroscopy. Pull-off test is used to evaluate the adhesion strength of the prepared coatings to the substrate, and field emission scanning electron microscopy is used for considering the fracture surface of the coated steel panels. The results clearly show that the corrosion resistance increases in the following order: pure epoxy < E-TCS0.1% < ECS2.5% < ECS-TCS0.5%, revealing that modifying the epoxy matrix with chitosan and loading the TCS in the epoxy coating increase the corrosion resistance more effectively through an eco-friendly approach and provide good anti-corrosion stability which is related to the chemical compatibility between the nanofiller and the matrix.

1. Introduction

Chitosan, a kind of N-deacetylated derivative of chitin, is a natural polymer with attractive inherent characteristics such as non-toxicity, biocompatibility, pH sensitivity, and low production cost [1–4]. The distinctive characteristics of chitosan are related to its amine (–NH_2) and hydroxyl (–OH) groups. These functional groups facilitate the structural modification, assist the hydrolysis and dissolve of chitosan under acidic aqueous media, and enhance the reaction of chitosan for providing homogeneous phases in chemical cross-linking networks. Moreover, it is proved that chitosan has anti-corrosive nature due to the coordination of chitosan with metal surface through –NH_2 and –OH groups [5–8].

Chitosan is regarded as an appropriate inhibitor for corrosion prevention in industries [9–12]. In a review paper, Ashassi-Sorkhabi and Kazempour [13] comprehensively introduced the chitosan and its derivatives for corrosion inhibition of steel alloys. In this regard, Fekry and Mohamed [14] reported that acetyl thiourea chitosan polymer is an effective inhibitor for decreasing the corrosion rate of the mild steel in 0.5 M H_2SO_4 solution through either decreasing the temperature or increasing the polymer concentration. El-Haddad [15] revealed that chitosan can be used as an inhibitor for cupper in 0.5 M HCl solution, which significantly decreases the cathodic, anodic and corrosion currents; according to this study, nitrogen and oxygen atoms in the molecular structure of chitosan are the main active sites for chitosan adsorption on the copper surface, and the thin layer of adsorbed chitosan and the complexes of chitosan molecules with Cu^{+} species reduce the corrosion rate of copper. Also, Zhang et al. [16] and Zhao et al. [17] synthesized chitosan derivatives for eco-friendly inhibition of corrosion on mild steel and carbon dioxide corrosion on P110 steel, respectively, and used theoretical calculations for investigating the chitosan adsorption mechanism.

Furthermore, the potential applications of chitosan based coatings for decreasing the corrosion rate of metallic structures have been investigated [13,18]. Ahmed et al. [19] showed that chitosan coated mild steel has good corrosion resistance in 0.5 M H_2SO_4, while glutaraldehyde can be used as a cross-linker for enhancing the mechanical strength of this coating. Zheludkevich et al. [20] prepared corrosion protective self-healing coatings consisted of a pre-layer of chitosan doped with cerium ions and a barrier hybrid film of titania-containing organic-inorganic hybrid sol-gel on an aluminum alloy surface. The cerium doped chitosan pre-layer can effectively improve the corrosion resistance due to the formation of complexes between cerium ions and functional groups of chitosan, and providing the prolonged-release of cerium ions. Besides, the chitosan has film-forming properties, acceptable adhesion to the metallic substrates and it can make complexes with corrosion inhibitors through reversible reactions. Ma et al. [5] used nano-chitosan as reinforcing agent in epoxy protective coatings on mild steel substrates, revealing that the nano-chitosan in epoxy/diamine would decrease the permeability of the coating, tortuous the diffusion path of corrosive agents, improve the adhesion of epoxy coating to the substrate, and improve the anti-corrosion properties.

Therefore, chitosan is a self-healing bio-polymer and corrosion inhibitor, and it can slow down the corrosion phenomenon in combination with protective barrier coatings [21–23], while it can be used for chemical modification and composite preparation in order to improve the inhibition properties [13,24]. The composites of inorganic nanomaterials with chitosan are another approach to utilize the advantages of chitosan and inorganic nanomaterials in order to increase the service-life of the polymer coatings via retarding the corrosion phenomenon. For example, John et al. [25] developed chitosan/TiO_2 nanocomposite coatings by sol-gel process on mild steel in order to decrease the mild steel corrosion in 0.1 N HCl solutions. Balaji and Sethuraman [26] synthesized chitosan doped organic-inorganic hybrid sol by hydrolysis and condensation of 3-glycidoxypropyltrimethoxy silane, tetraethoxysilane, and titanium isopropoxide in an acidic media for coating on aluminum substrate. The high corrosion protection of this process can be assigned to the covalent bonds of TiO_2 nanoparticles with surface –OH groups and silanol groups, and the dense adhesive chitosan coating with three dimensional network on the metal substrate. Ruhi et al. [27] developed epoxy coatings with higher corrosion resistance through loading chitosan-polypyrrole-SiO_2 composites in the epoxy matrix. They proved that the chemical interactions between the chitosan and the polypyrrole improve the integrity of the polymer matrix, and the SiO_2 particles reinforce the chitosan-polypyrrole matrix. Sambyal et al. [28] studied the effects of poly(aniline-anisidine)/chitosan/SiO_2 composites as nanofiller in the epoxy matrix, and showed that composites of SiO_2 nanoparticles, chitosan, and poly(aniline-anisidine) conductive polymer could be used for enhancing the barrier resistance of epoxy-based coatings. Majidi et al. [29] used the ternary hybrids of graphene oxide with ZnO and chitosan for corrosion protection of mild steel in 1.0 M HCl solution.

On the other hand, inorganic nanomaterials such as SiO_2 [30,31], TiO_2 [32,33], and halloysite nanotubes [34,35] are effective nanofillers for overcoming the shortcomings of the polymer matrix [36]. Meanwhile, TiO_2 nanostructures have received a noticeable attention in materials science due to possessing inherent properties such as non-toxicity, environment friendly, biocompatibility, anti-bacterial behavior, chemical and physical stability, high chemical inertness and high corrosion protection [37–40]. According to a study by Vijayan et al. [32], the TiO_2 nanotubes and natural halloysite nanotubes can be used as epoxy monomer reservoirs and theses reservoirs could be loaded in the epoxy coatings to achieve self-healing performance. Their results proved that the nature, surface area and diameter of the nanotubes are key factors for controlling the self-healing behavior and stability of epoxy coatings, and the TiO_2 nanotubes with higher surface area and lower tube diameter are superior in providing higher corrosion resistant coatings.

Although epoxy resins are extensively applied in different industries for providing corrosion protection of metallic structures, their barrier performance is vulnerable to various parameters including mechanical damages, hydrolytic degradation, and permeation of corrosive electrolyte through the coating pores [41–44]. Therefore, in this research, our main goal is to utilize the advantages of both chitosan and TiO_2 nanotubes for developing epoxy nanocomposite coatings with higher corrosion resistance. The effects of using chitosan solution and chitosan modified TiO_2 nanotubes on the anti-corrosion properties of epoxy coatings in NaCl corrosive electrolyte are investigated by salt spray test and electrochemical impedance spectroscopy.

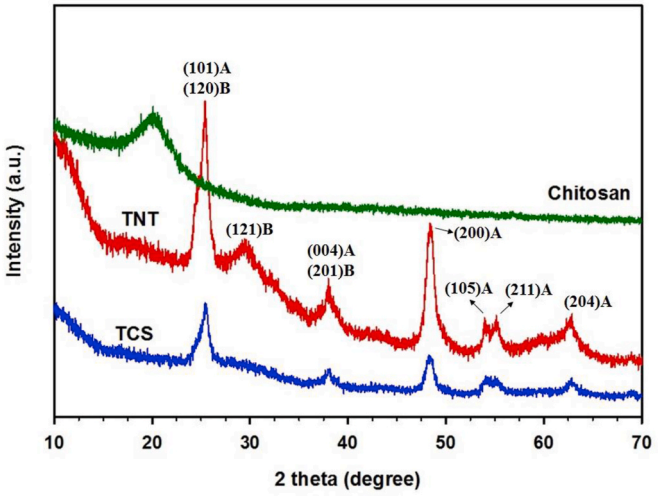

Fig. 1. XRD patterns of chitosan powder, TNT, and TCS.

2. Experimental

2.1. Materials

Glacial acetic acid (99%, Sinopharm Chemical Reagent Co.), chitosan (M_W = 300 kDa, Shanghai Macklin Biochemical Co.), Epoxy resin (Bisphenol A diglycidyl ether, solvent-based, epoxy equivalent = 0.41–0.48 mol/100 g, Viscosity = 6–10 Pa s, Feicheng Deyuan Chemicals Co.), phenolic aldehyde amine hardener (T31, Amine value = 450–550 KOH mg/g, Viscosity = 1–3 Pa s, Relative density = 1.01–1.10, Zhenjiang Danbao Resin Co., Ltd.), and thinner (PPG thinner #91–92, solvent-based, mixture of various components (such as xylene, isobutanol, ethylbenzene, and others), PPG Protective and Marine Coatings Industries, Inc.) were supplied and used without further purification treatments.

2.2. Synthesis of chitosan modified TiO_2 nanotubes

The TiO_2 nanotubes (abbreviated as TNT) were synthesized according to our previous study [45]. In a typical procedure for modifying the TNT with chitosan, 1 g TNT was dispersed in 50 mL of 1% v/v aqueous acetic acid and homogenized in an ultrasonic bath for 60 min. Besides, 1 g chitosan was dissolved in 100 mL of 1% v/v acetic acid through vigorous stirring at 45 ± 5 °C for 4 h. Then, chitosan solution was poured into the previously homogenized TNT dispersion, and stirred at 80 ± 5 °C for 24 h to obtain chitosan modified TNT which is abbreviated as TCS. The reaction products were centrifuged at 8000 rpm for 5 min, then washed with deionized water till pH = 7 to remove excess chitosan and acetic acid, and finally dried at 60 °C. The dried sample were ground to fine powders for further use.

2.3. Fabrication of epoxy coatings containing TCS

100 g epoxy resin and 20 g hardener were mixed thoroughly and diluted with thinner for making pure epoxy sample which is abbreviated as PE. Meanwhile, composite epoxy coatings containing different amounts of TCS (0.1, 0.5 and 1.0 wt%) were prepared and abbreviated as E-TCS0.1%, E-TCS0.5%, and E-TCS1.0%, respectively. For preparing the nanocomposite coatings, the required amounts of nanomaterials were homogeneously dispersed in thinner by bath ultrasonic treatment for 2 h. Next, the well-dispersed nanomaterials were added to the preheated epoxy resin at 70 ± 5 °C (to decrease the viscosity of epoxy resin), and vigorously stirred (on a hot-plate magnetic stirrer at speed of 1500 rpm) for 2 h to prepare homogenized mixture while turning off the heater during stirring to gradually reaching to room temperature (T_{room}). In the next step, the stoichiometric amount of the hardener was poured into the mixture and vigorously stirred for 10 min at T_{room}. The mixture was degassed, brush-painted on the cleaned Q235 steel substrates, dried at T_{room} for 1week and finally cured at 80 °C for 90 min.

2.4. Fabrication of epoxy coatings modified with chitosan

For preparing epoxy coatings modified with chitosan (abbreviated as ECS), 1 g chitosan powder was completely dissolved in 50 mL of 2% v/v

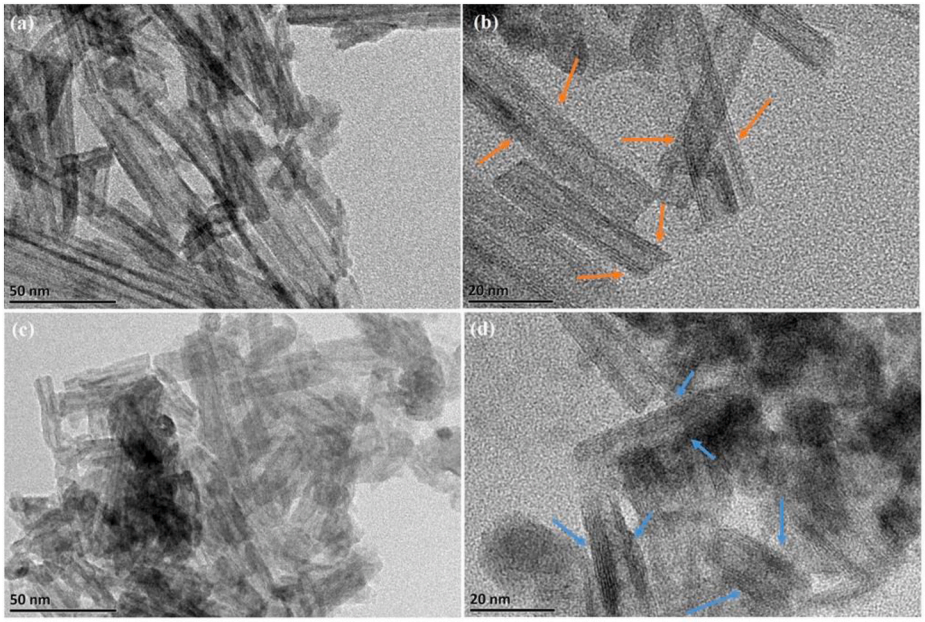

Fig. 2. TEM images of the synthesized (a, b) TNT and (c, d) TCS. The red arrows in Fig. 2(b) indicate the smooth and distinguishable edges of the TNT, while the blue arrows in Fig. 2(d) show the unclear and rough edges of the TCS. (For interpretation of the references to color in this figure legend, the reader is referred to the Web version of this article.)

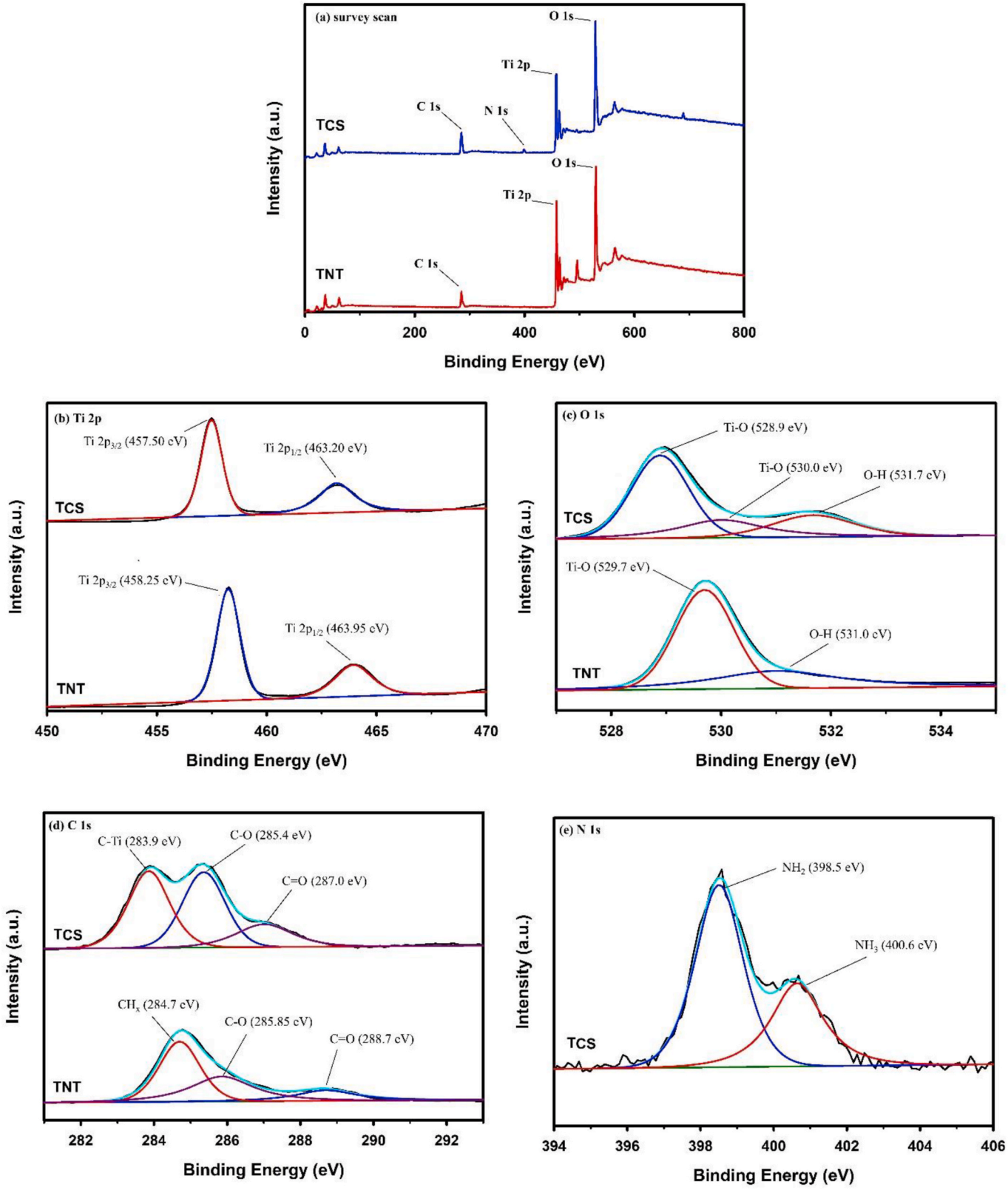

Fig. 3. XPS results of the synthesized TNT and TCS: (a) survey scan, and high resolution (b) Ti 2p, (c) O 1s, (d) C 1s, and (e) N 1s.

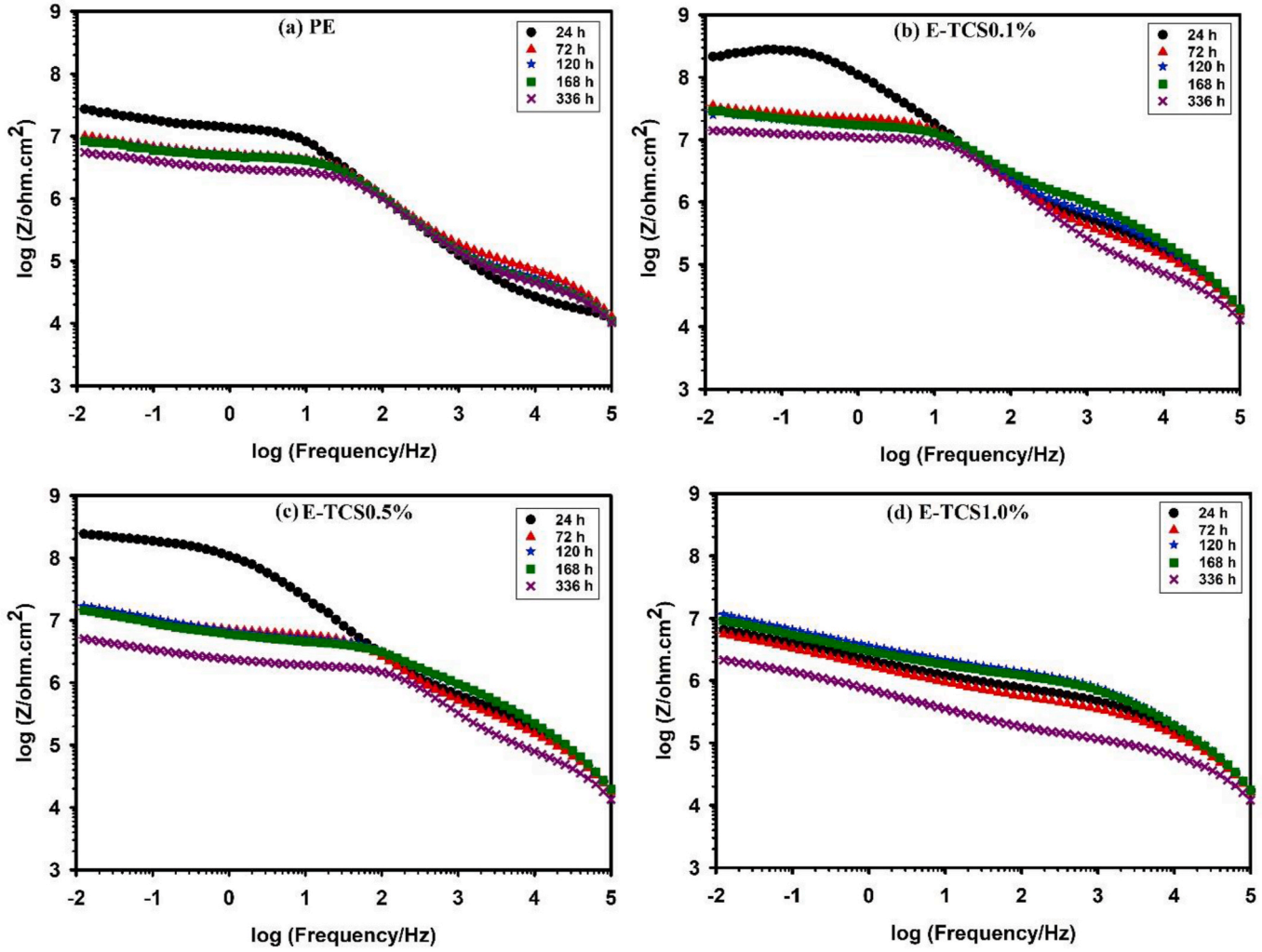

Fig. 4. Bode plots of (a) PE, (b) E-TCS0.1%, (c) E-TCS0.5%, and (d) E-TCS1.0%.

acetic acid solution under continuous stirring at 45 ± 5 °C for 4 h. Then, epoxy coatings modified with 1 and 2.5 wt% of aqueous chitosan solution were prepared by mixing chitosan solution with epoxy resin, which are abbreviated as ECS1% and ECS2.5%, respectively. The required amount of the chitosan solution was added to 100 g epoxy resin pre-heated at 70 ± 5 °C in an oil bath, and the mixture was continuously stirred at 70 ± 5 °C for 2 h. The transparent color of epoxy resin changes to milky in the first moments of adding chitosan, and then, the color of the epoxy resin changes back to its transparency after completely dissolving the chitosan in the epoxy resin. Next, the thinner was added to the epoxy/chitosan mixture at 70 ± 5 °C, and stirred for 30 min while turning off the heater to gradually reaching to T_{room}. Then, 20 g hardener was added to the prepared mixture and stirred continuously at T_{room}. The prepared composition was degassed, paint-brushed on the cleaned Q235 steel substrates, dried at T_{room} for 1week and finally cured at 80 °C for 90 min.

2.5. Fabrication of ECS coatings containing TCS

Since ECS2.5% showed slightly higher corrosion resistance compared to PE and ECS1% samples, the ECS2.5% sample was loaded with different amounts (0.1, 0.25, 0.5, and 1.0 wt%) of TCS abbreviated as ECS-TCS0.1%, ECS-TCS0.25%, ECS-TCS0.5%, and ECS-TCS1.0%, respectively. First, the required amounts of chitosan solution (as described in section 2.4) was added to the epoxy resin pre-heated at 70 ± 5 °C in an oil bath, and the mixture was continuously stirred at 70 ± 5 °C for 2 h. In another beaker, the required amounts of nanomaterials were uniformly dispersed in thinner by use of bath ultrasonic treatment for 2 h. Next, the dispersion of the nanomaterials in the thinner was added to the prepared epoxy/chitosan mixture at 70 ± 5 °C, and vigorously stirred for 2 h to prepare homogenized mixture while turning off the heater during stirring to gradually reaching to T_{room}. In the next step, the stoichiometric amount of the hardener was poured into the mixture while stirring for 10 min at T_{room}. The prepared composition was degassed, paint-brushed on the cleaned Q235 steel substrates, dried at T_{room} for 1week and finally cured at 80 °C for 90 min.

2.6. Characterization

The structures of the nanomaterials were studied by X-ray powder diffraction (XRD, Rigaku Ultima IV, Japan) with irradiation of Cu Kα at 40 kV and 40 mA in 2θ range of 10–70°, and X-ray photoelectron spectroscopy (XPS, Thermo Fisher Escalab 250Xi Multifunctional X-ray Spectrometer) with X-ray source of Al Kα (1486.68 eV). The synthesized TNT and TCS samples were grounded in agar mortar to have a fine powders to carry on the XRD and XPS analysis on them. Transmission electron microscopy (TEM, JEM-2100) was used for investigating the morphology of the nanopowders. The nanopowders were dispersed in absolute ethanol by the help of the bath-ultrasonic treatment and drop-coated on the carbon grids of the TEM, followed by drying in air at room

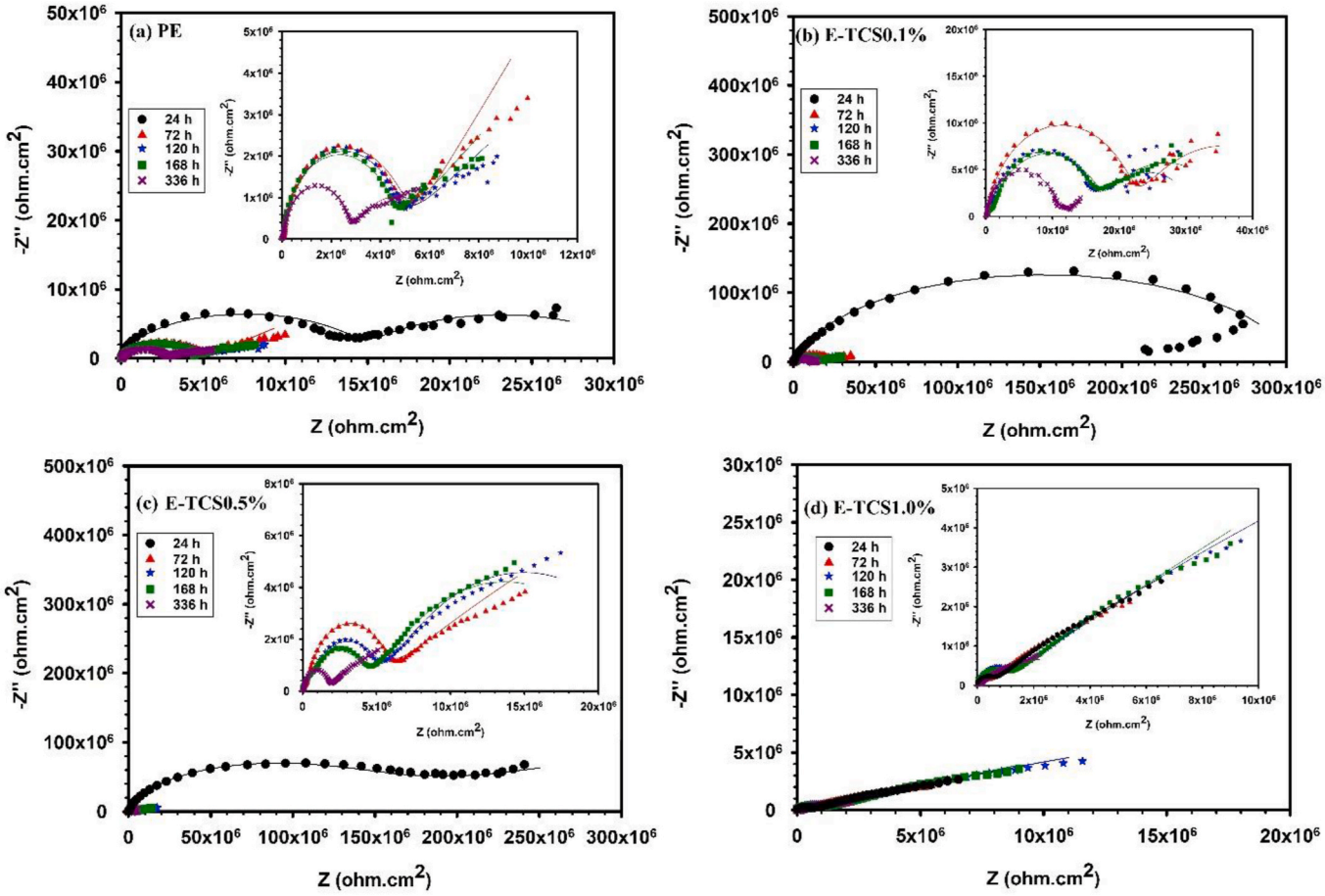

Fig. 5. Nyquist plots of (a) PE, (b) E-TCS0.1%, (c) E-TCS0.5%, and (d) E-TCS1.0%.

temperature in order to prepare the samples for TEM analysis.

Electrochemical impedance spectroscopy (EIS) and salt spray test were utilized to investigate the corrosion behavior of the prepared coatings. Samples with dry film thickness of 60 ± 10 μm were selected for corrosion studies. It should be mentioned that the coating thickness was determined using a digital coating thickness gauge (GTS8202, Guangzhou GuoOu Electronic Technology Co.). The EIS data were measured by a Potentiostat/Galvanostat (AMETEK Parstat, Princeton Applied Research, 4000+) with an electrode cell consisting of the coated substrate immersed in a 3.5 wt% NaCl solution (working electrode), Ag/AgCl electrode (reference electrode), and graphite rod (counter electrode). The EIS test was run when the open circuit potential (OCP) was steady and the frequency range of 10^5–10^{-2} Hz with 20 mV amplitude was used for recording the EIS curves. The obtained results were fitted by ZSimpWin (version 3.60) software. Beside the intact coatings, the EIS test was performed to evaluate the corrosion behavior of the coated samples with an artificial defect of 3 cm in length and the other EIS measurement conditions were similar to the intact coatings. It should be mentioned that the artificial defects are created in the middle of the coating samples by using a sharp knife through the coating to the metal substrate. The salt spray test was done based on ASTM B-117, and the coated steel panels were put in the salt spray chamber under the situation of 5 wt% NaCl solution at 35 ± 2 °C and 100% relative humidity for 500 h. The panels were scratched in X shape condition to accelerate the corrosion and the salt was sprayed for 1 min every 6 min. The specimens of salt spray test were evaluated via visual examinations. The pull-off adhesion test (DeFelsko, PosiTest, automatic) was performed according to ASTM D4541 to consider the adhesion strength of the coatings on the steel substrates. Field emission scanning electron microscopy (FE-SEM, MIRA3, TESCAN) was utilized to evaluate the fracture surface of the coatings.

3. Results and discussion

3.1. Characterization of nanomaterials

Fig. 1 shows the XRD patterns of the chitosan powder, TNT, and TCS. The XRD pattern of the chitosan powder shows a peak at 2θ = 20°, which is related to the semi-crystalline structure of the chitosan [46–48]. The main characteristic peaks of the TNT have appeared at 2θ of 25.4, 37.8, 48.5, 54.1, 55.3, 62.3, and 62.6°, which are assigned to the (120), (004), (200), (105), (211), (213), and (204) diffraction planes of TiO_2 anatase phase (JCPDS # 21–1272), while the peaks at 2θ of 25.4, 29.4, and 37.8° are also related to the (120), (121), and (201) diffraction planes of TiO_2 brookite phase (JCPDS # 29–1360). Since the main peaks of the TNT are attributed to the anatase phase, anatase is the major phase and brookite is the minor phase in its structure. In the case of TCS sample, the main characteristic peaks are observed at 2θ of 25.5, 38.1, 48.5, 54.0, 55.3, and 62.7°, which are related to the (101), (112), (200), (105), (211), and (204) diffraction planes of TiO_2 anatase phase (JCPDS # 21–1272). The crystalline peak of the chitosan is not observed in the XRD pattern of the synthesized TCS, while the diffraction pattern of the TCS is similar to the TNT and the intensities of the TCS peaks are lower than the intensities of the related peaks in the XRD pattern of the TNT; suggesting that the chitosan modification method has not destroyed the crystalline structure of the TNT and the chitosan is attached on the TNT through formation of hydrogen bonds and substitution of hydroxyl and amino-groups [49–51].

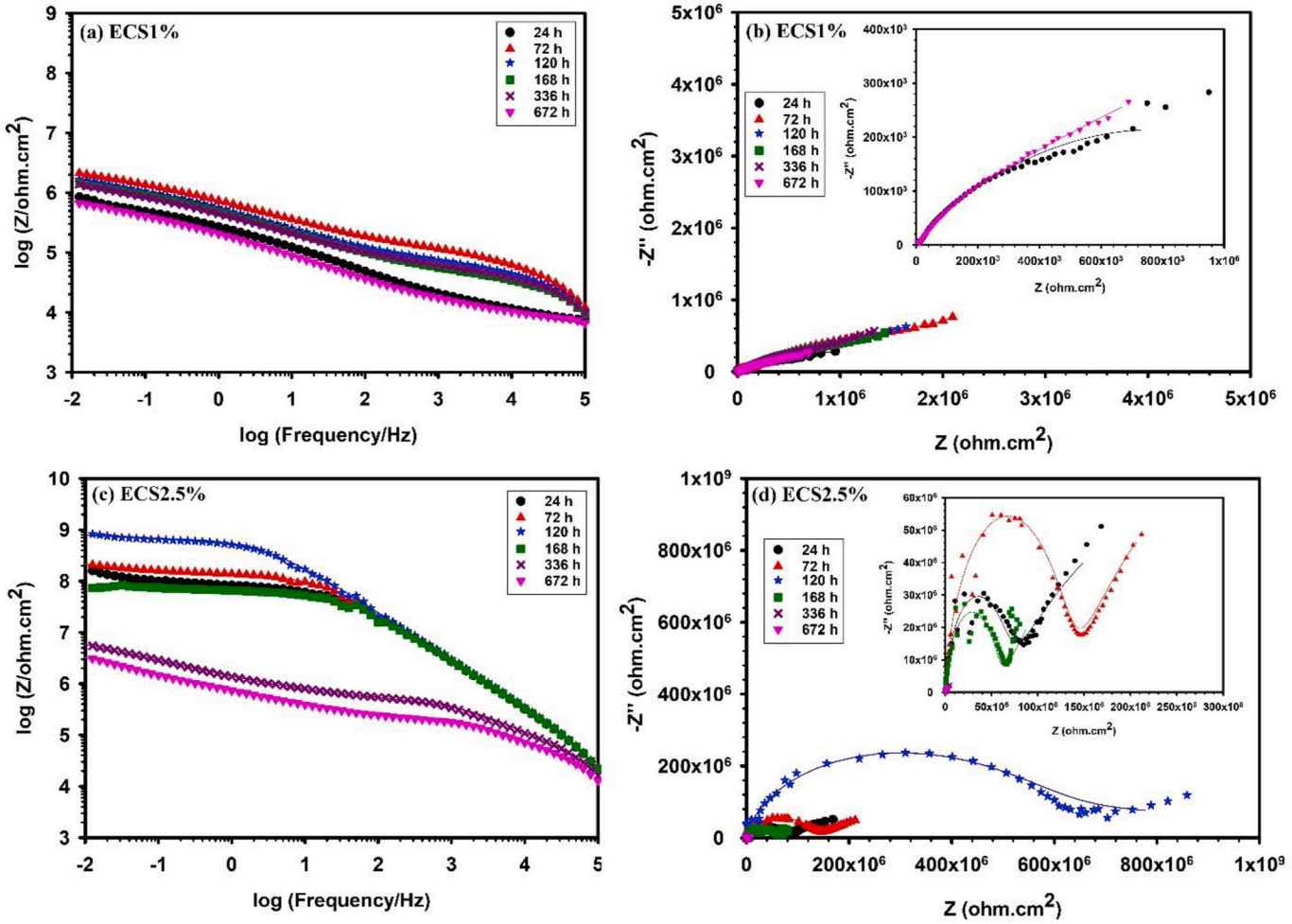

Fig. 6. Bode and Nyquist plots of (a, b) ECS1% and (c, d) ECS2.5%.

The TEM images in Fig. 2(a and b) confirm the TNT synthesis with the diameter of less than 10 nm and the length of 50–100 nm. Fig. 2(c and d) shows that in the case of TCS, a layer of chitosan polymer is grafted on the whole surface of TNT; i.e. the synthesized TNT has smooth surface with clear edges, while the nanotubes in TCS are rough with less distinguishable edges [52].

The XPS spectra of the TNT and TCS are shown in Fig. 3 to study the reaction of chitosan molecules with TNT. According to the survey scan presented in Fig. 3(a), Ti, O, and C elements are detected in both TNT and TCS, while the element of N is only found in the TCS. The Ti 2p high-resolution spectra of TNT (Fig. 3(b)) shows peaks at 458.25 and 463.95 eV which are related to Ti $2p_{3/2}$ and Ti $2p_{1/2}$, respectively. After grafting chitosan on TNT, the corresponding peaks are shifted to lower binding energies and appear at 457.5 and 463.2 eV, respectively [53,54]. As Fig. 3(c) shows, the O 1s spectrum of TNT is deconvoluted into two peaks at 529.7 and 531.0 eV, assigned to Ti–O and O–H, respectively. Meanwhile the O 1s spectrum of TCS is decomposed to peaks at 528.9, 530.0, and 531.7 eV, attributed to Ti–O, Ti–O, and O–H, respectively [55]. Fig. 3(d) indicates that the TNT sample features three C 1s peaks at 284.7, 285.85, and 288.7 eV, assigned to the CH_x, C–O, and C═O bonds, respectively, due to the presence of carbonate impurities absorbed on the TNT surface [56,57]. The C 1s spectrum of TCS can be deconvoluted into peaks at 283.9, 285.4, and 287.0 eV, related to C–Ti, C–O, and C═O or -C-O bonds, respectively [38,58]. Moreover, the N 1s high-resolution spectrum of TCS (Fig. 3(e)) is fitted into two peaks at 398.5 and 400.6 eV, related to $–NH_2$ and protonated $–NH_3^+$ groups in chitosan, respectively [38]. The results of XPS indicate that there is a strong interaction between TNT and chitosan and chitosan is grafted on the surface of TNT in the TCS sample.

3.2. Characterization of coatings

The coating performance and the degradation respect to the immersion time in corrosive media is studied by EIS. The various Bode plots recorded by EIS test of PE and E-TCS series (E-TCS0.1%, E-TCS0.5%, and E-TCS1.0%) after immersion in 3.5 wt% NaCl solution are presented in Fig. 4(a–d), while their corresponding Nyquist plots are shown in Fig. 5(a–d). The low-frequency impedance modulus ($|Z|_{0.01Hz}$) for PE sample is 27.5, 10.5, 8.9, 8.2, and 5.6 MΩ cm^2 after immersion for 24, 72, 120, 168, and 336 h, respectively. In the case of E-TCS0.1% sample, the $|Z|_{0.01Hz}$ values after the above-mentioned immersion times are 228.8, 35.9, 27.1, 29.9, and 14.3 MΩ cm^2, respectively; indicating that the corrosion resistance improves by adding 0.1 wt% TCS to the epoxy matrix compared to the pure sample. However, the corrosion resistance decreases by increasing the amounts of TCS into the epoxy matrix which could be attributed to the agglomeration of the nanoparticles within the epoxy matrix [59,60]. The $|Z|_{0.01Hz}$ values of 250.2, 15.5, 18.2, 15.2, and 5.3 MΩ cm^2 are recorded for E-TCS0.5% and the $|Z|_{0.01Hz}$ values of 7, 5.8, 12.3, 9.7, and 2.2 MΩ cm^2 are obtained for E-TCS1.0% after 24, 72, 120, 168, and 336 h immersion, respectively. Therefore, the corrosion resistance in the E-TCS coating systems enhances as the following order: E-TCS1.0% < E < E-TCS0.5% < E-TCS0.1%.

The chitosan is used to chemically modify the epoxy matrix in order

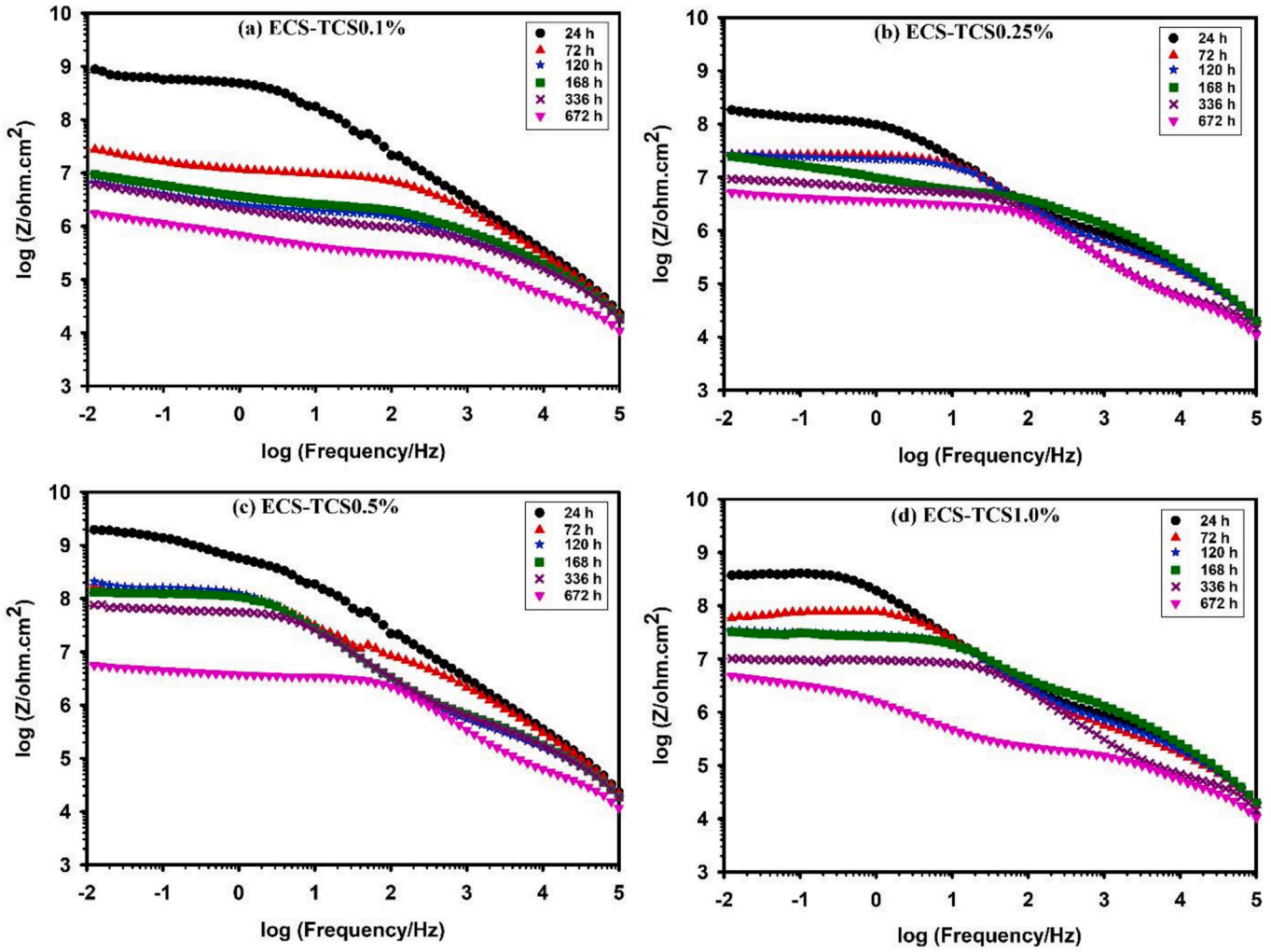

Fig. 7. Bode plots of (a) ECS-TCS0.1%, (b) ECS-TCS0.25%, (c) ECS-TCS0.5%, and (d) ECS-TCS1.0%.

to achieve better chemical compatibility between epoxy matrix and TCS nanofillers. Chitosan solution in amounts of 1 and 2.5 wt% are loaded into the epoxy resin to select the appropriate chitosan amount and the developed ECS coatings are evaluated by EIS tests. Fig. 6 shows the EIS results for ECS1% and ECS2.5%, revealing that the amount of chitosan solution in epoxy resin is an important factor controlling the corrosion resistance of the coatings. The Bode and Nyquist plots clearly show that the ECS2.5% has higher impedance modulus and corrosion resistance than ECS1%, and the $|Z|_{0.01Hz}$ values for ECS2.5% after 24, 72, 120, 168, 336, and 672 h immersion are 176, 217, 86.7, 76.1, 5.8, and 3.4 MΩ cm^2, respectively. The impedance modulus of ECS2.5% sample increases during immersion time and then, the impedance modulus decreases by prolonging the corrosion test. The decrease of corrosion resistance by prolonging the immersion time is due to the permeation of the corrosive ions into the coating and reaching to the interface of the coating and the substrate. Meanwhile, the increase of the coating resistance for the ECS samples during the first days of immersion can be attributed to the modification of epoxy matrix with chitosan solution; i.e. the chitosan acts as corrosion inhibitor and prevents the corrosive agents permeation into the coating through blocking the pores of the coating by corrosion products [5].

Then, the epoxy coatings modified with 2.5 wt% chitosan solution are loaded with different wt.% of TCS nanofillers (ECS-TCS series of coatings), and their corresponding Bode and Nyquist plots are represented in Fig. 7 and Fig. 8, respectively. The results clearly show that the ECS-TCS0.5% sample could provide significantly higher corrosion resistance during immersion in NaCl solution compared to the other ECS-TCS samples and the values of $|Z|_{0.01Hz}$ after 24, 72, 120, 168, 336, and 672 h immersion are 1952, 186, 227, 133, 80.7, and 5.8 MΩ cm^2, respectively.

To compare the samples, the samples with the highest corrosion resistance from each series (PE, E-TCS, ECS, and ECS-TCS) are selected and the $|Z|_{0.01Hz}$ values versus immersion time are depicted in Fig. 9(a). Moreover, the electrical equivalent circuits (EECs) shown in Fig. 9(b) are used for fitting the EIS data to quantify the corrosion resistance of the coating system and the Chi-square range of the fitting results is 9×10^{-3} - 7×10^{-4}. The EEC includes the resistance of the solution (R_s), the resistance of the coating (R_{coat}), the constant phase element of the coating (CPE_{coat}), the resistance against the charge transfer (R_{ct}), and the constant phase element of the double layer (CPE_{dl}). The Warburg finite diffusion impedance element is an additional diffusion component presented in Fig. 9(b-II), related to the corrosive agents diffusion in the pores and defects of the coating; while the diffusion components including the constant phase element of the corrosion products (CPE_{diff}) and the resistance of the corrosion products (R_{diff}) have appeared in Fig. 9(b-III) and Fig. 9(b-IV) due to the formation and agglomeration of the corrosion products at the interface of the coating and the metal substrate. The EEC shown in Fig. 9(b-I) is used for fitting the EIS results of all the samples (PE, E-TCS0.1%, ECS2.5%, and ECS-TCS0.5%) after 24 h immersion, and the other EECs are applied for EIS fitting after increasing the immersion time. The EEC in Fig. 9(b-II) is only used for fitting the EIS data of PE after 48 h immersion and the EEC in Fig. 9(b-III)

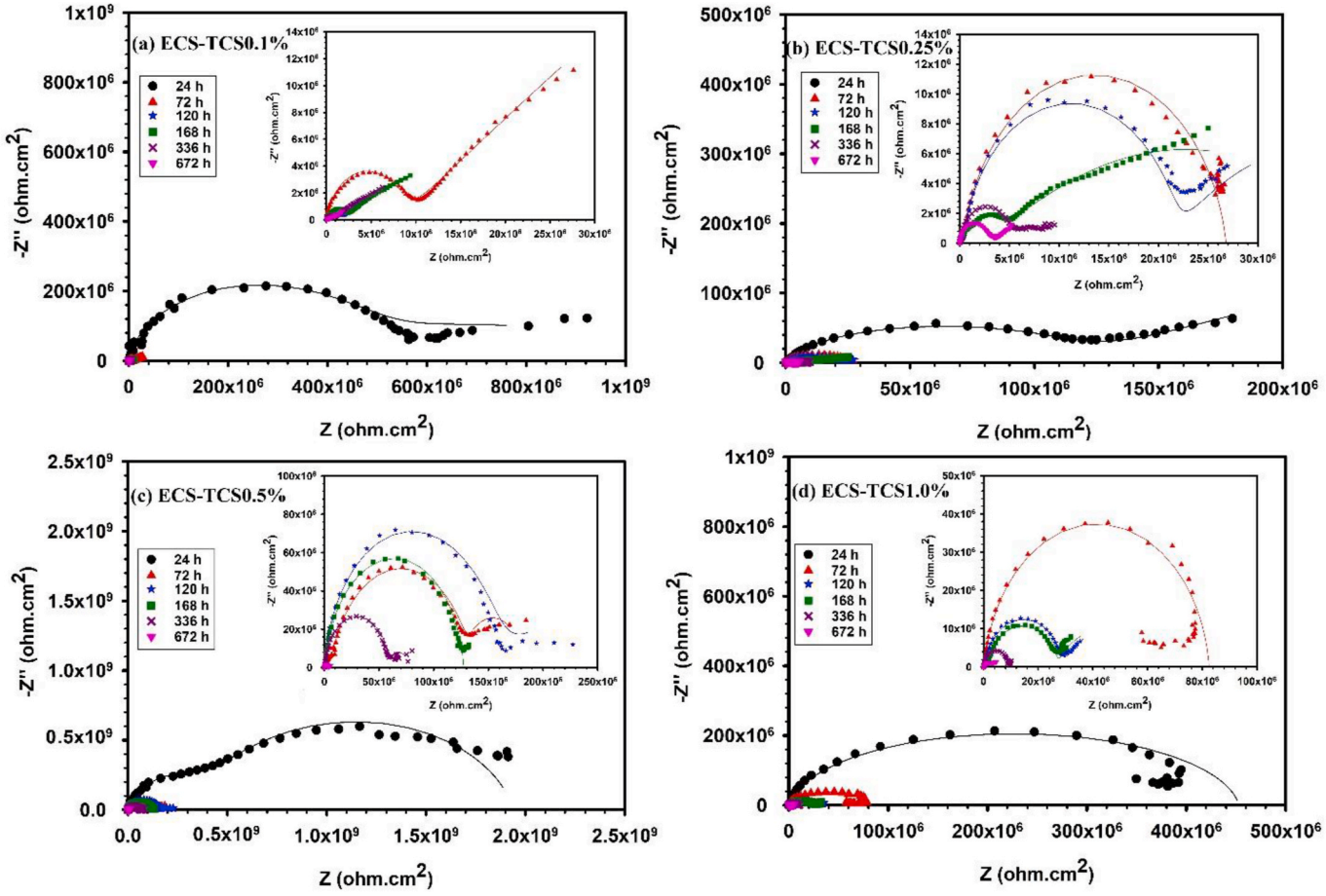

Fig. 8. Nyquist plots of (a) ECS-TCS0.1%, (b) ECS-TCS0.25%, (c) ECS-TCS0.5%, and (d) ECS-TCS1.0%.

is used for fitting the EIS curves of PE during other days of immersion. The corrosion behavior of ECS2.5% sample is considered by Fig. 9(b-III), while Fig. 9(b-IV) is adapted for investigating the corrosion behavior of E-TCS0.1% and ECS-TCS0.5% samples by increasing the immersion time. Since the EECs have 2 and 3 time constants, it can be concluded that the corrosive media has reached to the interface of the coating with metal substrate during the first hours of immersion.

According to the results presented in Fig. 9, the samples show complicated behavior during immersion time; meanwhile, the order of corrosion resistance increases as follows: PE < E-TCS0.1% < ECS2.5% < ECS-TCS0.5%. The $|Z|_{0.01Hz}$ values for PE and E-TCS0.1% decrease steadily by increasing the immersion time, whereas, the $|Z|_{0.01Hz}$ values for ECS2.5% and ECS-TCS0.5% show a fluctuating trend which are finally lower than the $|Z|_{0.01Hz}$ values for the initial hours of immersion. The amounts of defects within the coating increase and the resistance of the coating decreases during the exposure time. Therefore, the corrosion protection performance and barrier resistance of the epoxy coatings can be improved by homogeneously dispersing the TCS nanomaterials in the epoxy coating. Moreover, when the chitosan in its pure form is added to the epoxy matrix, it provides moderate corrosion protection and the corrosion resistance decreases significantly after immersion for 336 h which is because of chitosan high tendency toward reaction with water and facilitating the electrolyte diffusion into the coating [61]. However, the modification of TNT with chitosan besides modifying the epoxy matrix with chitosan is a more appropriate approach for enhancing the properties of the epoxy coatings against corrosion phenomenon [13]. The TCS and chitosan act as interlocking points in the epoxy coating and decrease the permeation of electrolyte into the coating and inhibit the corrosion reactions [28].

Also, the values of R_{diff} for modified epoxy coatings (i.e. E-TCS0.1%, ECS2.55, and ECS-TCS0.5%) are higher than PE sample during immersion time, indicating that uniform layer of corrosion products with chitosan backbone have covered the substrate surface. The higher R_{diff} values of nanocomposite coatings is assigned to the presence of chitosan in the prepared nanocomposites; because the functional groups of chitosan act as nucleation sites for growth of iron oxides and corrosion products. This uniform layer would act as an extra-protective complex layer on the substrate surface [61].

The EIS results and the variation of $|Z|_{0.01Hz}$ during immersion time (i.e. 2, 24, 48, 72, and 96 h) for coated substrates with artificial defects are presented in Fig. 10 and Fig. 11, respectively, to study the corrosion phenomenon at the interface of the coating and the metal substrate. The PE sample shows a continuous decline in the impedance values during immersion which indicates that the corrosive agents including water, oxygen, and corrosive ions have penetrated into the coating and the corrosion reactions under the scratched coating has proceeded which is because of coating delamination and losing the chemical bond between the coating and the steel substrate. The other composite samples have higher impedance modulus than PE and the corrosion protection performance improves as: PE < E-TCS0.1% < ECS2.5% < ECS-TCS0.5%, revealing that composite coatings could provide higher barrier protection. The higher $|Z|_{0.01Hz}$ values for ECS2.5% and ECS-TCS0.5% compared to E-TCS0.1% sample indicates the importance of adding chitosan into the polymer matrix which can successfully decrease the diffusion of the electrolyte through the defects of the matrix into the interface of the coating with the substrate as well as improving the chemical compatibility between the TCS and the epoxy. Indeed, the dispersion quality of nanomaterials in the matrix and the adhesion

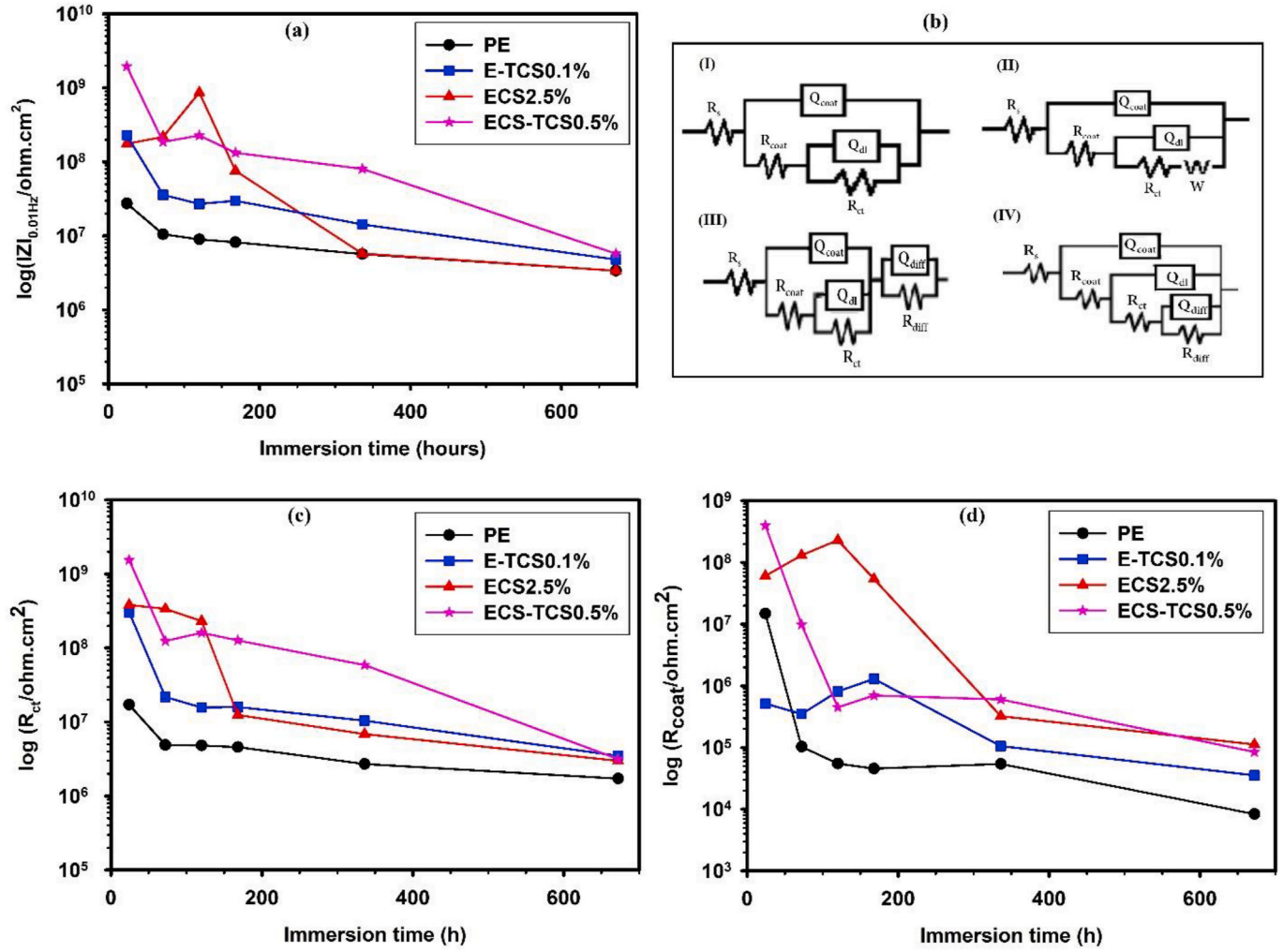

Fig. 9. (a) The variation of $|Z|_{0.01Hz}$ as a function of immersion time in 3.5 wt% NaCl solution for PE, E-TCS0.1%, ECS2.5%, and ECS-TCS0.5%. (b) The EECs used for fitting the EIS results of coated substrates. The calculated values of (c) R_{ct} and (d) R_{coat} during immersion in 3.5 wt% NaCl solution.

strength between the nanofiller and the matrix could be controlled by the chemical reactions between the nanofillers and the polymer matrix [62–64]. Meanwhile, the variation of the impedance modulus during immersion time for the composite coatings is different from the PE sample and they do not show continuous decline in impedance modulus by prolonging the immersion time; i.e. the impedance modulus of composite samples decreases during the first 48 h of immersion, and then, their impedance modulus increases by prolonging the immersion time to 72 h immersion, followed by a decrease trend in impedance through increasing the immersion time to 96 h. Indeed, the results indicate that the chitosan acts as a corrosion inhibitor [65], and as Atay et al. [21] revealed, the homogeneous chitosan solution dissolved in acid solutions could be loaded as self-healing agent in the epoxy polymer. Accordingly, it seems that the chitosan slightly shows self-healing performance by the increase of the impedance values during immersion intervals.

Furthermore, salt spray test is used to visually evaluate the corrosion of the prepared nanocomposite coatings. Fig. 12 represents the images of samples after salt spray test. In the case of PE sample, the corrosion products have covered the coating surface near the X-cut, while the corrosion products near the X-cut of E-TCS0.1% sample is significantly lower than that of PE. The coating delamination happens as a result of corrosive media diffusion into the interface of the coating with the metal surface through the ascribe mark [66]. Moreover, the ECS-TCS0.5% shows higher corrosion protection when exposed to the high humidity and high salt content in the salt chamber, because negligible amounts of corrosion products can be seen near the scratch; this behavior can be assigned to the synergistic effects of chitosan molecules and TCS nanofiller in the epoxy matrix.

The results of pull-off adhesion test under dry and wet (672 h immersion in 3.5 wt% NaCl solution) conditions are shown in Fig. 13. The detachment of PE sample in both dry and wet conditions is adhesive failure. The other coatings show higher adhesion strength to the steel substrate with cohesive failure in dry test and adhesive failure in wet test. Meanwhile, epoxy coatings modified with chitosan (i.e. ECS2.5% and ECS-TCS0.5%) show better performance compared to both PE and E-TCS0.1%, which can be attributed to the effect of chitosan on the epoxy adhesion to the steel substrate; indeed, the chitosan inherently has $–NH_2$ and –OH groups which can increase the binding strength of the coating to the steel substrate, while the O and N atoms have corrosion inhibition effects on the steel [61,67].

Fig. 14 shows the FE-SEM images from the fracture surface of the prepared coatings. The PE sample (Fig. 14(a)) shows brittle fracture with smooth fracture surface and cracks in different planes [68]. The EP fracture surface is porous, while the composite coatings show different behavior and their fracture surfaces seem to be denser. In Fig. 14(b), the small well-dispersed dots would be assigned to both the end of the TCS in the polymer matrix and the chitosan grafting on the TNTs; in this regard, Zhang et al. [69] reported similar fracture surface for epoxy coatings loaded with chitosan modified carbon nanotubes. In the case of

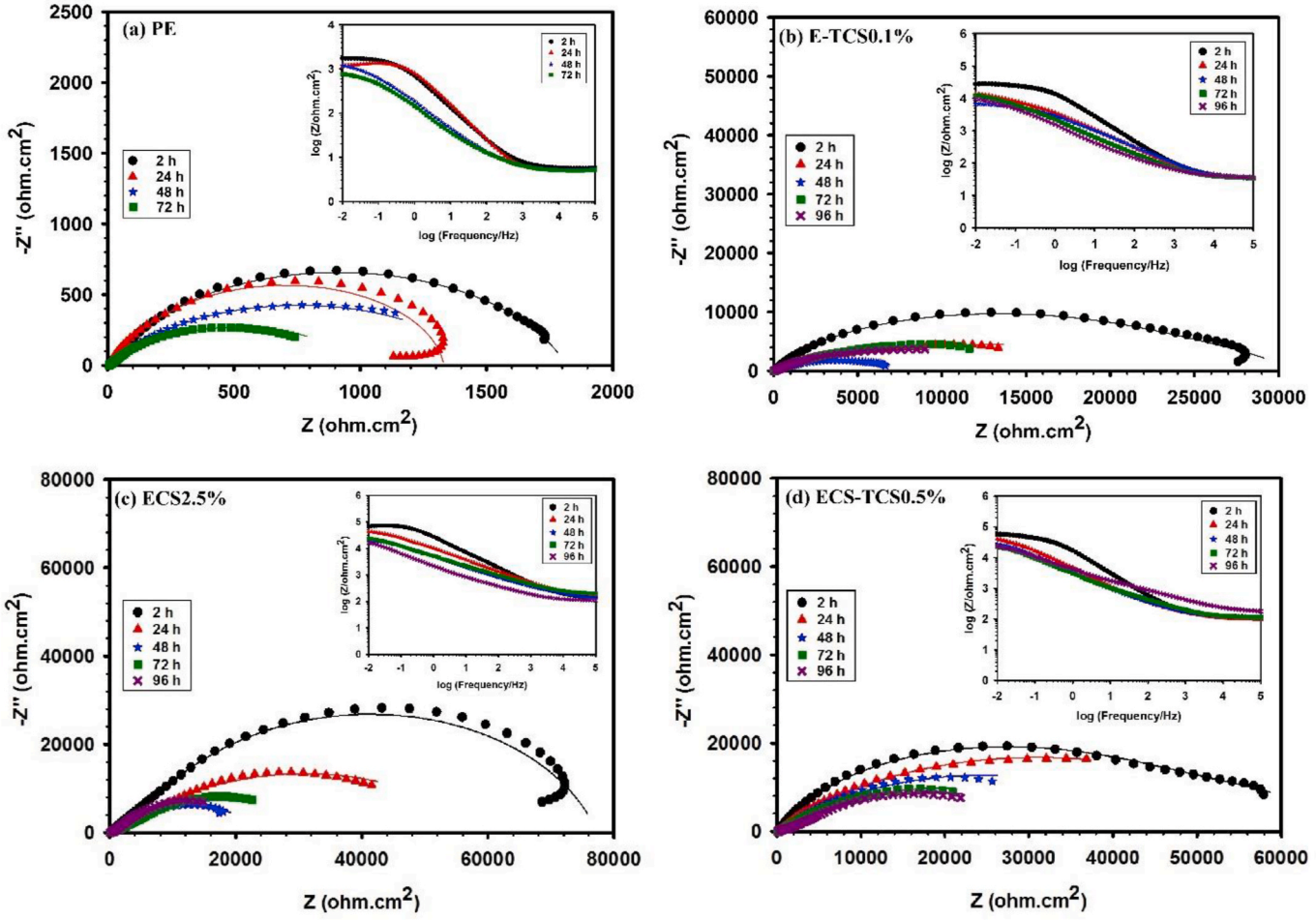

Fig. 10. The Nyquist and Bode plots of coated samples with artificial scratch during immersion in 3.5 wt% NaCl solution: (a) PE, (b) E-TCS0.1%, (c) ECS2.5%, and (d) ECS-TCS0.5%.

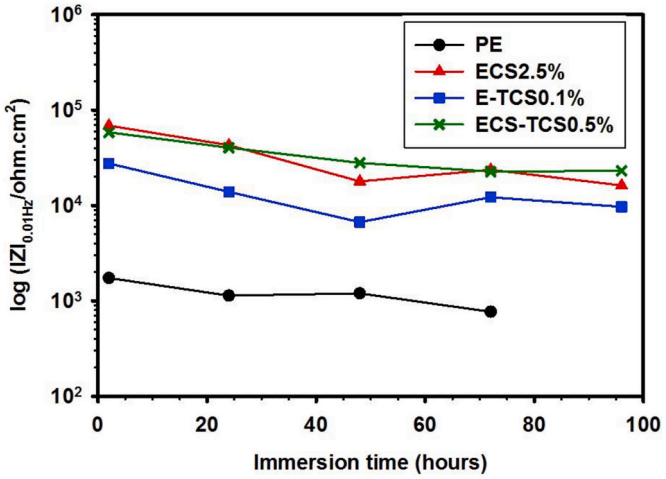

Fig. 11. The variation of impedance modulus at low frequency of 0.01 Hz as a function of immersion time in 3.5 wt% NaCl solution for PE, E-TCS0.1%, ECS2.5%, and ECS-TCS0.5% samples with artificial defect.

ECS2.5% (Fig. 14(c)), the chitosan in the epoxy matrix appears as spheres which are homogeneously blended in the epoxy coating. The homogeneous granular dispersion is because of chemical interactions between the chitosan functional groups and the epoxy [70,71]. When Fig. 14(d) is compared with Fig. 14(b), the ECS-TCS0.5% shows evenly dispersion of TCS nanofillers in the polymer matrix and no holes and cracks can be observed, indicating that the nanofillers and the polymer matrix have stronger interactions with uniform interface through loading the TCS in the chitosan modified epoxy matrix. Furthermore, the nanofillers have not pull out of the matrix upon fracture and no aggregates emerges on the cross-section surface, revealing a high interfacial adhesion between the matrix and nanofillers because of their high chemical compatibility [72]. Meanwhile, in comparison to Fig. 14(c), loading TCS in the chitosan modified epoxy matrix could decrease the porosity and cracks in the matrix, while the flocculation has disappeared.

3.3. Corrosion protection mechanism

The polymer coatings protect the metallic substrates from corrosion through barrier performance, while the nanocomposite coatings can delay the corrosion phenomenon by limiting the access of corrosive agents (i.e. water, oxygen, and chloride ions) to the interface of the coating with metal substrate. When nanofillers are added into the epoxy in appropriate wt.%, they can increase the diffusion path and improve the barrier performance of the coatings [66,73,74].

In this research, in the case of E-TCS coating systems, the chitosan on the surface of TNT can act as a bridge between the TCS and the epoxy matrix, improving the corrosion resistance which is further proved by Shi et al. [75].

Epoxy coatings loaded with 2.5% chitosan solution show higher impedance modulus in the initial hours of immersion time due to

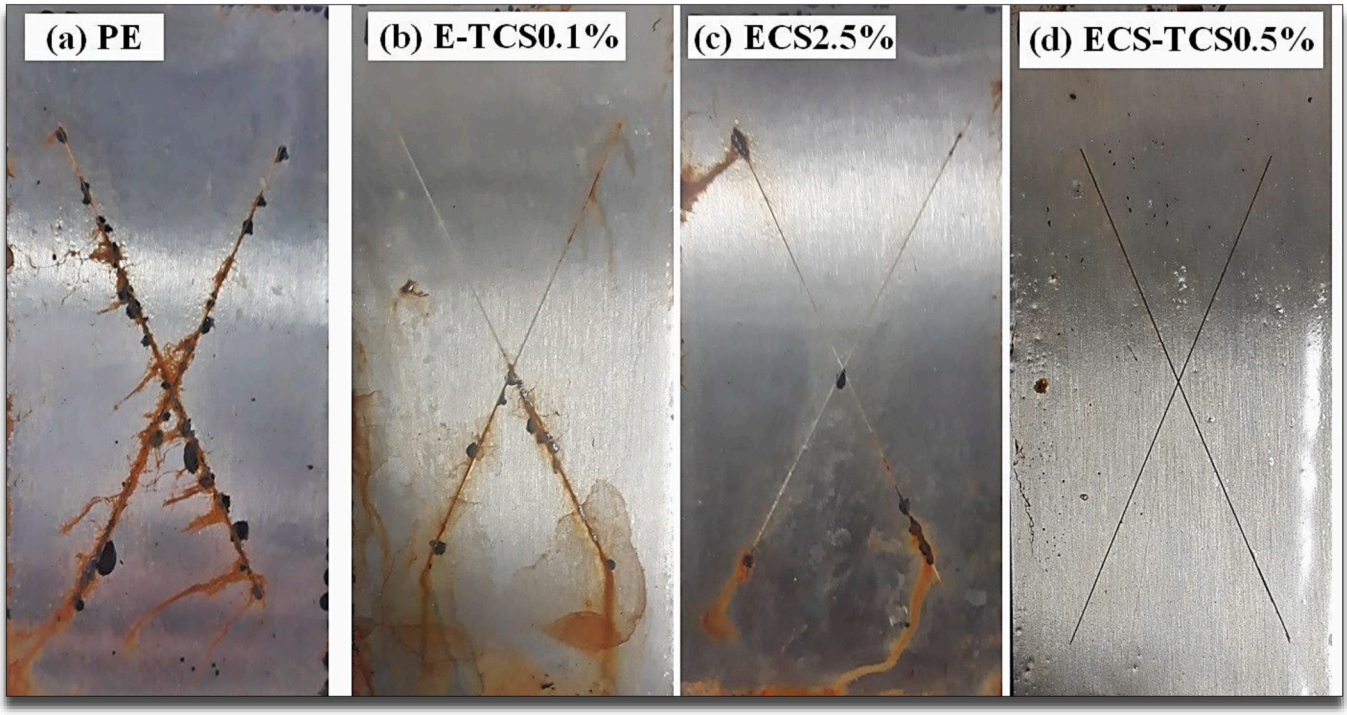

Fig. 12. Images from coated samples after 500 h salt spray test.

covalent bonding between the oxirane groups of epoxy with amino groups of chitosan producing an intrachain network. Moreover, the nitrogen and oxygen atoms of chitosan as well as epoxy matrix can make strong bonds with the π-electrons of the substrate surface, and block the active carrion sites at the interface of the coating with the metal substrate [5,6]. However, chitosan has hydrophilic nature and its amine and hydroxyl groups are active sites for water absorption [70,76]; therefore, the corrosion resistance of ECS2.5% decreases by prolonging the immersion time and reaches to almost the same impedance modulus of PE sample.

Meanwhile, the higher corrosion resistance of ECS-TCS0.5% sample is related to the mutual effects achieved by chitosan excellent film forming capability and TCS reinforcing tendency within epoxy matrix. It should be mentioned that the free –OH groups of chitosan are responsible for water absorption and when chitosan is used for modifying the epoxy matrix and the surface of TNT, the free –OH groups of chitosan are not available due to taking part in chemical reactions between polymer matrix and nanofillers; therefore, nanocomposites would uptake less water [27,77]. Furthermore, the corrosion products on the substrate coated with PE are agglomerated and form clusters of corrosion products on the steel; however, when chitosan is used as modifying agent for nanofillers and epoxy coating, it can prevent the corrosion products agglomeration on the metal surface through steric stabilization approach and therefore, a uniform corrosion layer is formed [61]. Besides, the TCS in the epoxy coating inhibits the electrolyte penetration into the interface of the coating with substrate and improves the coating barrier resistance. Therefore, the epoxy matrix modified with chitosan and loaded with TCS nanofillers has the potential for postponing the corrosion reactions and provide higher corrosion protection performance.

Moreover, a comparison between the achievements in this research and the other related researches is provided in Table 1 to pave the way for future studies. In Table 1, the optimum corrosion protection efficiency is calculated based on Equation (1), in order to facilitate the comparison between different coating systems:

$$corrosion\ protection\ efficiency\% = \frac{(|Z|_{0.01Hz}^{nanocomposite\ coating}) - (|Z|_{0.01Hz}^{pure\ coating})}{|Z|_{0.01Hz}^{pure\ coating}} \quad (1)$$

where, the $|Z|_{0.01Hz}^{pure\ coating}$ and $|Z|_{0.01Hz}^{nanocomposite\ coating}$ are the low-frequency impedance values recorded for the pure polymer coatings and the nanocomposite coatings, respectively.

4. Conclusion

In summary, TNT in anatase phase is hydrothermally synthesized, and chemically modified with aqueous chitosan solution (TCS). The structure and morphology of the synthesized TNT and TCS are studied by XRD, XPS, and TEM analysis. Then, three different categories of epoxy composite coatings are prepared as follows: (1) the epoxy composite coatings loaded with different wt.% (0.1, 0.5, and 1.0 wt%) of TCS as nanofiller, (2) the epoxy coatings modified with 1 and 2.5 wt% of aqueous chitosan solution as polymer matrix modifier, and (3) the epoxy coatings modified with 2.5 wt% of aqueous chitosan solution and loaded with different wt.% (0.1, 0.25, 0.5, and 1.0 wt%) of TCS. The corrosion protection performance of the prepared composite coatings are evaluated by EIS and salt spray test, while the adhesion strength of the coatings to the metallic substrates are measured by pull-off adhesion test. The results reveal that the wt.% of nanofillers or chitosan solution

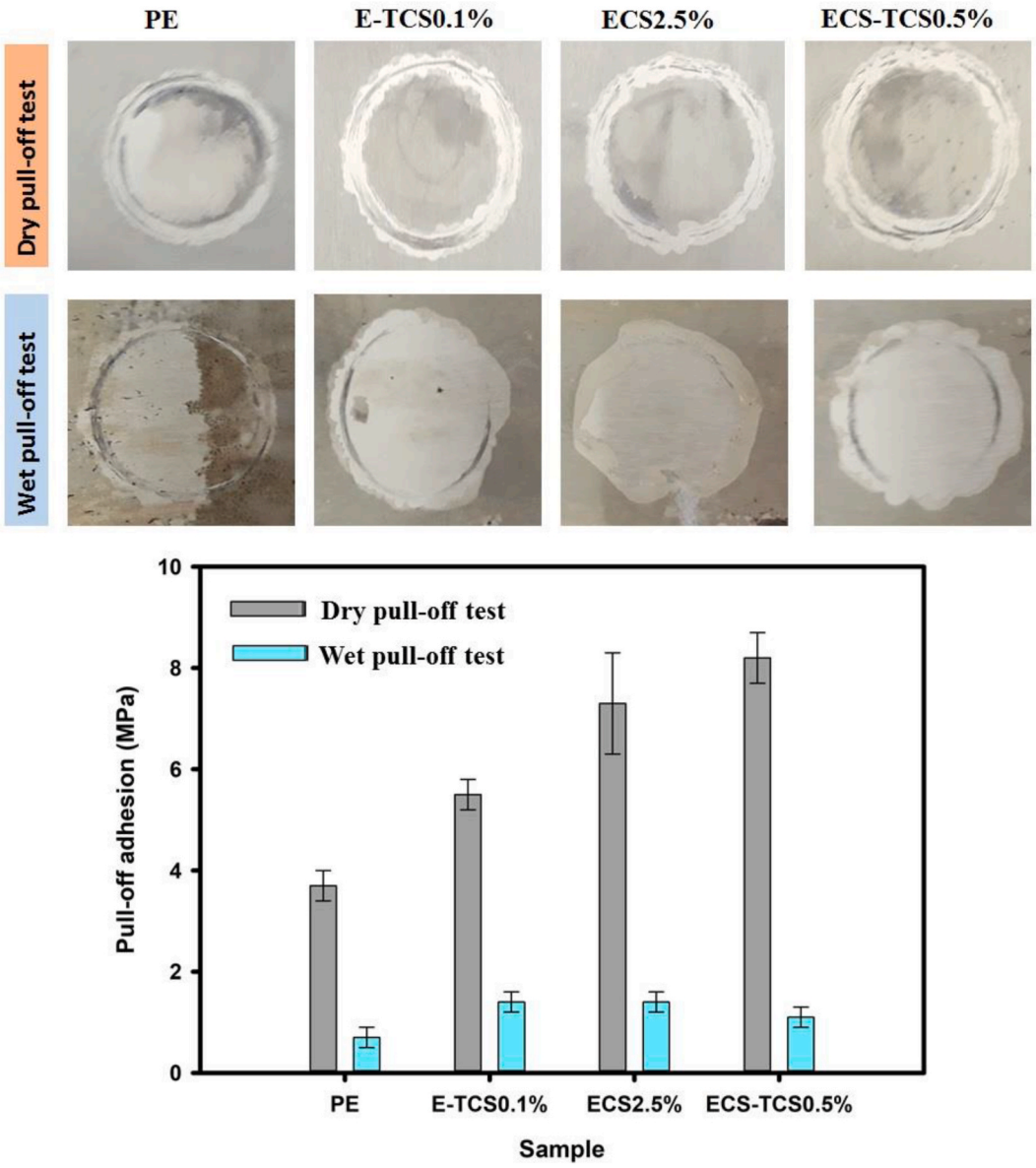

Fig. 13. The images of pull-off detaching status and the quantitative pull-off adhesion results for dry and wet (672 h immersion in 3.5 wt% NaCl solution) samples.

have great effect on the properties of the composite coatings, and meanwhile, the ECS-TCS0.5% coating (i.e. the epoxy matrix is modified with 2.5 wt% aqueous chitosan solution and loaded with 0.5 wt% TCS nanofillers) has the highest protection against corrosion and the highest adhesion strength both in dry and wet pull-off tests compared to the other composite coatings. Indeed, when both the polymer matrix is modified with the chitosan solution and the TNT is chemically modified with the chitosan, the chemical compatibility between the polymer matrix and the nanofillers enhances. Hence, the chitosan acts as a bridging between the nanofiller and the epoxy matrix which could provide higher barrier effects and passivate the metal surface, leading to decrease in the degradation of coating under corrosive environment. This research paves the way for utilizing the properties of natural and non-toxic chitosan polymer in anti-corrosion nanocomposite coatings through both ways of modifying the nanofillers and improving the polymer matrix with chitosan polymer.

CRediT authorship contribution statement

Sepideh Pourhashem: Conceptualization, Investigation, Methodology, Writing – original draft, Writing – review & editing, Funding acquisition. **Jizhou Duan:** Conceptualization, Supervision, Writing – review & editing, Funding acquisition. **Ziyang Zhou:** Investigation, Writing – original draft, Writing – review & editing. **Xiaohong Ji:** Investigation, Writing – original draft, Writing – review & editing. **Jiawen Sun:** Investigation. **Xucheng Dong:** Investigation. **Lifei Wang:** Investigation, Resources. **Fang Guan:** Investigation, Resources. **Baorong Hou:** Supervision.

Declaration of competing interest

The authors declare that they have no known competing financial interests or personal relationships that could have appeared to influence the work reported in this paper.

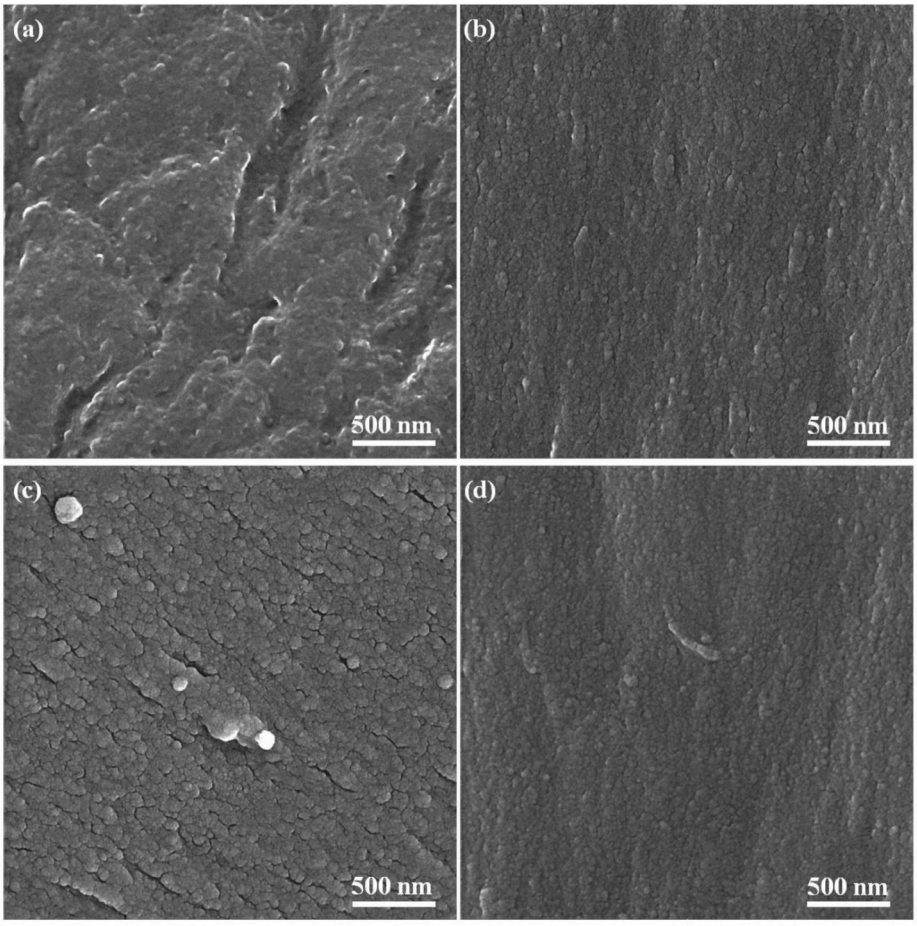

Fig. 14. FE-SEM images from fracture surface of (a) PE, (b) E-TCS0.1%, (c) ECS2.5%, and (d) ECS-TCS0.5%.

Table 1
A comparison between the corrosion protection performance of the coating developed in this research and the results revealed by other researchers in this field.

Polymer matrix	Modifying agent for polymer matrix	Optimum Nanofiller	Metallic substrate	Coating thickness (μm)	Optimum corrosion protection efficiency (%)	Initial immersion time	Optimum corrosion protection efficiency (%)	Final immersion time	Reference
Epoxy	–	TiO_2 nanotubes encapsulated with epoxy pre-polymer	Steel	300	–	–	99.6%	96 h	[32]
Polydimethyl siloxane	–	TiO_2 nanoparticles (8 wt%)	Aluminum alloy	–	90%	30 min	Only data for nanocomposite sample is given (for 40 days of immersion) which is not comparable with pure coating.		[78]
Waterborne epoxy	–	Meso-TiO_2 nanoparticles (0.56 wt %)	Steel	50 ± 5	57.4%	0 h	28.5%	720 h	[79]
Epoxy	–	TiO_2 nanogel (0.1–3.0 wt%)	Steel	100	The corrosion protection behavior is studied by salt spray. The pure epoxy coating fails after 500 h salt spray, while nanocomposite coatings preserve their protection even after 1000 h salt spray test.				[80]
Epoxy	–	TiO_2 nano-containers loaded with 8-hydroxy-quinoline (1 wt%)	Aluminum alloy	–	82.7%	24 h	Still good corrosion protection	247 h	[81]
Epoxy	Chitosan solution (20 wt%)	–	Steel	60 ± 5	The corrosion protection behavior is studied by salt spray. The pure epoxy coating fails after 500 h, while nanocomposite coatings preserve their protection after 500 h salt spray test.				[6]
Epoxy	Chitosan solution	–	–	–	Self-healing performance				[21]
Solvent- based epoxy	Chitosan solution (2.5 wt%)	Chitosan modified TiO_2 nanotubes (0.5 wt%)	Steel	60 ± 10	98.5%	24 h	41.2%	672 h	This research

Acknowledgement

The present work is supported financially by CAS President's International Fellowship Initiative (PIFI, No. 2019PE0059), and CAS-VPST Silk Road Science Fund 2021 (133137KYSB20200034).

References

[1] T. Li, et al., Chitosan and graphene oxide nanocomposites as coatings for controlled-release fertilizer, Water, Air, Soil Pollut. 230 (7) (2019) 146.
[2] Y. Liu, et al., β-Cyclodextrin modified natural chitosan as a green inhibitor for carbon steel in acid solutions, Ind. Eng. Chem. Res. 54 (21) (2015) 5664–5672.
[3] S.S. Behera, et al., Chitosan/TiO2 composite membrane improves proliferation and survival of L929 fibroblast cells: application in wound dressing and skin regeneration, Int. J. Biol. Macromol. 98 (2017) 329–340.
[4] Y. Haldorai, J.J. Shim, Novel chitosan-TiO2 nanohybrid: preparation, characterization, antibacterial, and photocatalytic properties, Polym. Compos. 35 (2) (2014) 327–333.
[5] I.W. Ma, et al., Anticorrosion properties of epoxy-nanochitosan nanocomposite coating, Prog. Org. Coating 113 (2017) 74–81.
[6] M. Abd El-Fattah, et al., Improvement of corrosion resistance, antimicrobial activity, mechanical and chemical properties of epoxy coating by loading chitosan as a natural renewable resource, Prog. Org. Coating 101 (2016) 288–296.
[7] X.T. Le, et al., Covalent grafting of chitosan onto stainless steel through aryldiazonium self-adhesive layers, ACS Appl. Mater. Interfaces 6 (12) (2014) 9085–9092.
[8] S. Yang, et al., Preparation and characterization of antibacterial electrospun chitosan/poly (vinyl alcohol)/graphene oxide composite nanofibrous membrane, Appl. Surf. Sci. 435 (2018) 832–840.
[9] J. Haque, et al., Microwave-induced synthesis of chitosan Schiff bases and their application as novel and green corrosion inhibitors: experimental and theoretical approach, ACS Omega 3 (5) (2018) 5654–5668.
[10] D.S. Chauhan, et al., Thiosemicarbazide and thiocarbohydrazide functionalized chitosan as ecofriendly corrosion inhibitors for carbon steel in hydrochloric acid solution, Int. J. Biol. Macromol. 107 (2018) 1747–1757.
[11] D.S. Chauhan, et al., Aminotriazolethiol-functionalized chitosan as a macromolecule-based bioinspired corrosion inhibitor for surface protection of stainless steel in 3.5% NaCl, Int. J. Biol. Macromol. 152 (2020) 234–241.
[12] K.E. Mouaden, et al., Thiocarbohydrazide-crosslinked chitosan as a bioinspired corrosion inhibitor for protection of stainless steel in 3.5% NaCl, Sustain. Chem. Pharm. 15 (2020), 100213.
[13] H. Ashassi-Sorkhabi, A. Kazempour, Chitosan, its derivatives and composites with superior potentials for the corrosion protection of steel alloys: a comprehensive review, Carbohydr. Polym. (2020), 116110.
[14] A. Fekry, R.R. Mohamed, Acetyl thiourea chitosan as an eco-friendly inhibitor for mild steel in sulphuric acid medium, Electrochim. Acta 55 (6) (2010) 1933–1939.
[15] M.N. El-Haddad, Chitosan as a green inhibitor for copper corrosion in acidic medium, Int. J. Biol. Macromol. 55 (2013) 142–149.
[16] Q. Zhang, et al., Two novel chitosan derivatives as high efficient eco-friendly inhibitors for the corrosion of mild steel in acidic solution, Corrosion Sci. 164 (2020), 108346.
[17] Q. Zhao, et al., Chitosan derivatives as green corrosion inhibitors for P110 steel in a carbon dioxide environment, Colloids Surf. B Biointerfaces 194 (2020), 111150.
[18] X. Pang, I. Zhitomirsky, Electrodeposition of composite hydroxyapatite–chitosan films, Mater. Chem. Phys. 94 (2–3) (2005) 245–251.
[19] R.A. Ahmed, R. Farghali, A. Fekry, Study for the stability and corrosion inhibition of electrophoretic deposited chitosan on mild steel alloy in acidic medium, Int. J. Electrochem. Sci. 7 (2012) 7270–7282.
[20] M. Zheludkevich, et al., Self-healing protective coatings with "green" chitosan based pre-layer reservoir of corrosion inhibitor, J. Mater. Chem. 21 (13) (2011) 4805–4812.
[21] H.Y. Atay, L.E. Doğan, E. Çelik, Investigations of self-Healing property of chitosan-reinforced epoxy dye composite coatings, J. Mater. 2013 (2013) 1–7.
[22] M. Odarczenko, et al., Self-protecting epoxy coatings with anticorrosion microcapsules, ACS Omega 3 (10) (2018) 14157–14164.
[23] E.M. Fayyad, et al., Oleic acid-grafted chitosan/graphene oxide composite coating for corrosion protection of carbon steel, Carbohydr. Polym. 151 (2016) 871–878.
[24] P. Dutta, R. Srivastava, J. Dutta, Functionalized nanoparticles and chitosan-based functional nanomaterials. Multifaceted development and application of biopolymers for biology, Biomed. Nanotechnol. (2012) 1–50.
[25] S. John, et al., Corrosion inhibition of mild steel using chitosan/TiO2 nanocomposite coatings, Prog. Org. Coating 129 (2019) 254–259.
[26] J. Balaji, M. Sethuraman, Chitosan-doped-hybrid/TiO2 nanocomposite based sol-gel coating for the corrosion resistance of aluminum metal in 3.5% NaCl medium, Int. J. Biol. Macromol. 104 (2017) 1730–1739.
[27] G. Ruhi, O. Modi, S. Dhawan, Chitosan-polypyrrole-SiO2 composite coatings with advanced anticorrosive properties, Synth. Met. 200 (2015) 24–39.
[28] P. Sambyal, et al., Enhanced anticorrosive properties of tailored poly (aniline-anisidine)/chitosan/SiO2 composite for protection of mild steel in aggressive marine conditions, Prog. Org. Coating 119 (2018) 203–213.
[29] H.J. Majidi, et al., Fabrication and characterization of graphene oxide-chitosan-zinc oxide ternary nano-hybrids for the corrosion inhibition of mild steel, Int. J. Biol. Macromol. 148 (2020) 1190–1200.
[30] G. Tang, et al., Preparation and anticorrosion resistance of a self-curing epoxy nanocomposite coating based on mesoporous silica nanoparticles loaded with perfluorooctyl triethoxysilane, J. Appl. Polym. Sci. (2020) 49072.
[31] W. Han, et al., Fracture toughness and wear properties of nanosilica/epoxy composites under marine environment, Mater. Chem. Phys. 177 (2016) 147–155.
[32] P. Vijayan, Y.M. Hany El-Gawady, M. Al-Maadeed, A comparative study on long term stability of self-healing epoxy coating with different inorganic nanotubes as healing agent reservoirs, Express Polym. Lett. 11 (11) (2017).
[33] M. Mahmoudian, et al., Effects of different polypyrrole/TiO2 nanocomposite morphologies in polyvinyl butyral coatings for preventing the corrosion of mild steel, Appl. Surf. Sci. 268 (2013) 302–311.
[34] P. Vijayan, Y.M. Hany El-Gawady, M.A.S. Al-Maadeed, Halloysite nanotube as multifunctional component in epoxy protective coating, Ind. Eng. Chem. Res. 55 (42) (2016) 11186–11192.
[35] Y. Jia, et al., Preparation of pH responsive smart nanocontainer via inclusion of inhibitor in graphene/halloysite nanotubes and its application in intelligent anticorrosion protection, Appl. Surf. Sci. 504 (2020), 144496.
[36] S. Pourhashem, et al., Polymer/Inorganic nanocomposite coatings with superior corrosion protection performance: a review, J. Ind. Eng. Chem. (2020).
[37] C. Arunchandran, et al., Self-healing corrosion resistive coatings based on inhibitor loaded TiO2 nanocontainers, J. Electrochem. Soc. 159 (11) (2012) C552.
[38] K. Karthikeyan, A. Nithya, K. Jothivenkatachalam, Photocatalytic and antimicrobial activities of chitosan-TiO2 nanocomposite, Int. J. Biol. Macromol. 104 (2017) 1762–1773.
[39] S. Jafari, et al., Biomedical applications of TiO2 nanostructures: recent advances, Int. J. Nanomed. 15 (2020) 3447.
[40] Y. Qing, et al., Facile fabrication of superhydrophobic surfaces with corrosion resistance by nanocomposite coating of TiO2 and polydimethylsiloxane, Colloid. Surface. Physicochem. Eng. Aspect. 484 (2015) 471–477.
[41] D.A. Bellido-Aguilar, et al., Solvent-free synthesis and hydrophobization of biobased epoxy coatings for anti-icing and anticorrosion applications, ACS Sustain. Chem. Eng. 7 (23) (2019) 19131–19141.
[42] J. Kim, et al., Fabrication and mechanical properties of carbon fiber/epoxy nanocomposites containing high loadings of noncovalently functionalized graphene nanoplatelets, Compos. Sci. Technol. (2020), 108101.
[43] O. Dagdag, et al., Fabrication of polymer based epoxy resin as effective anti-corrosive coating for steel: computational modeling reinforced experimental studies, Surfaces. Interface. 18 (2020), 100454.
[44] A.M. Kumar, et al., Hierarchical graphitic carbon nitride-ZnO nanocomposite: viable reinforcement for the improved corrosion resistant behavior of organic coatings, Mater. Chem. Phys. 251 (2020), 122987.
[45] S. Pourhashem, et al., New effects of TiO2 nanotube/g-C3N4 hybrids on the corrosion protection performance of epoxy coatings, J. Mol. Liq. 317 (2020), 114214.
[46] M. Jaiswal, V. Koul, A.K. Dinda, In vitro and in vivo investigational studies of a nanocomposite-hydrogel-based dressing with a silver-coated chitosan wafer for full-thickness skin wounds, J. Appl. Polym. Sci. 133 (21) (2016).
[47] M. Anand, et al., Synthesis of chitosan nanoparticles by TPP and their potential mosquito larvicidal application, Front. Lab. Med. 2 (2) (2018) 72–78.
[48] L. Li, et al., Preparation of graphene oxide/chitosan complex and its adsorption properties for heavy metal ions, Green Process. Synth. 9 (1) (2020) 294–303.
[49] A. Morlando, et al., Suppression of the photocatalytic activity of TiO2 nanoparticles encapsulated by chitosan through a spray-drying method with potential for use in sunblocking applications, Powder Technol. 329 (2018) 252–259.
[50] M.H. Farzana, S. Meenakshi, Synergistic effect of chitosan and titanium dioxide on the removal of toxic dyes by the photodegradation technique, Ind. Eng. Chem. Res. 53 (1) (2014) 55–63.
[51] B. Li, et al., Synthesis, characterization, and antibacterial activity of chitosan/TiO2 nanocomposite against Xanthomonas oryzae pv. *oryzae*, Carbohydrate Poly. 152 (2016) 825–831.
[52] R. Zhai, et al., Chitosan–halloysite hybrid-nanotubes: horseradish peroxidase immobilization and applications in phenol removal, Chem. Eng. J. 214 (2013) 304–309.
[53] A. Al-Mokaram, et al., The development of non-enzymatic glucose biosensors based on electrochemically prepared polypyrrole–chitosan–titanium dioxide nanocomposite films, Nanomaterials 7 (6) (2017) 129.
[54] B. Sun, et al., Controlled fabrication of Sn/TiO 2 nanorods for photoelectrochemical water splitting, Nanoscale. Res. Lett. 8 (1) (2013) 462.
[55] Z. Hamden, et al., In situ generation of TiO2 nanoparticles using chitosan as a template and their photocatalytic activity, J. Photochem. Photobiol. Chem. 321 (2016) 211–222.
[56] Y. Bai, et al., Higher UV-shielding ability and lower photocatalytic activity of TiO 2@ SiO 2/APTES and its excellent performance in enhancing the photostability of poly (p-phenylene sulfide), RSC Adv. 7 (35) (2017) 21758–21767.
[57] A. Moya, et al., Large area photoelectrodes based on hybrids of CNT fibres and ALD-grown TiO 2, J. Mater. Chem. 5 (47) (2017) 24695–24706.
[58] P.-C. Li, et al., Fabrication and characterization of chitosan nanoparticle-incorporated quaternized poly (vinyl alcohol) composite membranes as solid electrolytes for direct methanol alkaline fuel cells, Electrochim. Acta 187 (2016) 616–628.
[59] S. Pourhashem, et al., Exploring corrosion protection properties of solvent based epoxy-graphene oxide nanocomposite coatings on mild steel, Corrosion Sci. 115 (2017) 78–92.

[60] T.T. Le, et al., Thermal, mechanical and antibacterial properties of water-based acrylic Polymer/SiO2–Ag nanocomposite coating, Mater. Chem. Phys. 232 (2019) 362–366.
[61] G.E. Luckachan, V. Mittal, Anti-corrosion behavior of layer by layer coatings of cross-linked chitosan and poly (vinyl butyral) on carbon steel, Cellulose 22 (5) (2015) 3275–3290.
[62] F.A. dos Santos, G.C. Iulianelli, M.I.B. Tavares, The use of cellulose nanofillers in obtaining polymer nanocomposites: properties, processing, and applications, Mater. Sci. Appl. 7 (2016) 257, 05.
[63] D. Pan, et al., Thermally Conductive Anticorrosive Epoxy Nanocomposites with Tannic Acid-Modified Boron Nitride Nanosheets, Industrial & Engineering Chemistry Research, 2020.
[64] K. Rajitha, K.N. Mohana, Application of modified graphene oxide–Polycaprolactone nanocomposite coating for corrosion control of mild steel in saline medium, Mater. Chem. Phys. 241 (2020), 122050.
[65] H. Ashassi-Sorkhabi, R. Bagheri, B. Rezaei-moghadam, Sonoelectrochemical synthesis of ppy-MWCNTs-chitosan nanocomposite coatings: characterization and corrosion behavior, J. Mater. Eng. Perform. 24 (1) (2015) 385–392.
[66] A.A. Javidparvar, R. Naderi, B. Ramezanzadeh, Manipulating graphene oxide nanocontainer with benzimidazole and cerium ions: application in epoxy-based nanocomposite for active corrosion protection, Corrosion Sci. 165 (2020), 108379.
[67] S.A. Umoren, et al., Inhibition of mild steel corrosion in HCl solution using chitosan, Cellulose 20 (5) (2013) 2529–2545.
[68] H.A. Al-Turaif, Effect of nano TiO2 particle size on mechanical properties of cured epoxy resin, Prog. Org. Coating 69 (3) (2010) 241–246.
[69] Y. Zhang, S. Huang, Significant improvements in the mechanical properties of chitosan functionalized carbon nanotubes/epoxy composites, RSC Adv. 6 (31) (2016) 26210–26215.
[70] S. Jabeen, et al., Influence of chitosan and epoxy cross-linking on physical properties of binary blends, Int. J. Polym. Anal. Char. 21 (2) (2016) 163–174.
[71] H.Y. Atay, E. Çelik, Investigations of antibacterial activity of chitosan in the polymeric composite coatings, Prog. Org. Coating 102 (2017) 194–200.
[72] S.-F. Wang, et al., Preparation and mechanical properties of chitosan/carbon nanotubes composites, Biomacromolecules 6 (6) (2005) 3067–3072.
[73] C.I. Idumah, et al., Recently emerging nanotechnological advancements in polymer nanocomposite coatings for anti-corrosion, anti-fouling and self-healing, Surfaces. Interface. (2020), 100734.
[74] S. Mohammadi, et al., Electrochemical and anticorrosion behavior of functionalized graphite nanoplatelets epoxy coating, J. Ind. Eng. Chem. 20 (6) (2014) 4124–4139.
[75] H. Shi, et al., Synthesis of carboxymethyl chitosan-functionalized graphene nanomaterial for anticorrosive reinforcement of waterborne epoxy coating, Carbohydr. Polym. (2020), 117249.
[76] S.A. Umoren, et al., Evaluation of chitosan and carboxymethyl cellulose as ecofriendly corrosion inhibitors for steel, Int. J. Biol. Macromol. 117 (2018) 1017–1028.
[77] F. Gao, et al., Fabrication of chitosan/heparinized graphene oxide multilayer coating to improve corrosion resistance and biocompatibility of magnesium alloys, Mater. Sci. Eng. C 104 (2019), 109947.
[78] X. Cui, et al., Polydimethylsiloxane-titania nanocomposite coating: fabrication and corrosion resistance, Polymer 138 (2018) 203–210.
[79] N. Wang, et al., Effect of different structured TiO2 particle on anticorrosion properties of waterborne epoxy coatings, Corrosion Eng. Sci. Technol. 51 (5) (2016) 365–372.
[80] A.M. Atta, et al., Epoxy embedded with TiO2 nanogel composites as promising self-healing organic coatings of steel, Prog. Org. Coating 105 (2017) 291–302.
[81] A. Balaskas, et al., Improvement of anti-corrosive properties of epoxy-coated AA 2024-T3 with TiO2 nanocontainers loaded with 8-hydroxyquinoline, Prog. Org. Coating 74 (3) (2012) 418–426.